Thy, P., Lesher, C.E, and Larsen, H.C. (Eds.)
Proceedings of the Ocean Drilling Program, Initial Reports Volume 163X

6. Transect EG65 Results[1]

Scientific Party[2]

SCIENTIFIC OBJECTIVES

The principal objective of drilling Transect EG65 was to sample volcanic basement formed during breakup and onset of seafloor spreading in a position midway between the plume track of Transect EG68 (Greenland-Iceland Rise) and the distal drilling sites of Transect EG63 (Ocean Drilling Program [ODP] Legs 152 and 163) (Fig. **F6**). The SIGMA survey shows that the maximum thickness of the volcanic crust changes northward between 64° and 66°N from 18–20 to 30–32 km. Importantly, by 66°N (SIGMA-II line), the maximum crustal thickness (~28 km) is close to the thickness imaged along the entire Greenland-Iceland Rise (SIGMA-I line) (Hollbrook et al., 2001). Likewise, the composition of basalts recovered by drilling along Transects EG66 (see the **"Transect EG66 Results"** chapter), EG68 (see the **"Transect EG68 Results"** chapter), and at Site ODP 988 have close affinities to those of Paleogene Iceland and the East Greenland flood basalt province, suggesting melt generation and differentiation under similar conditions. Given the coherence of these relationships, we viewed the area of transitional crust between 64° and 66°N as the highest priority for drilling because work here could provide the critical samples to directly relate changes in crustal structure to processes of mantle melt generation and crustal accretion.

The goal of Transect EG65 drilling was to sample above and below the break-up unconformity and to recover material from the youngest portions of the seaward-dipping reflector sequences feasible with our drilling system (i.e., without sediment cover). Based on the excellent coverage by the H/S *Dana* survey, a transect at 65°N was selected that closely followed seismic Line DLC9709 (Fig. **F1**). This seismic line (Fig. **F2**) shows key structural elements in the uppermost crust with an inner continental basement high and an outer igneous plateau with strong seaward-dipping reflectors separated by a prebreak-up sedimentary ba-

F1. Transect EG65 area, p. 26.

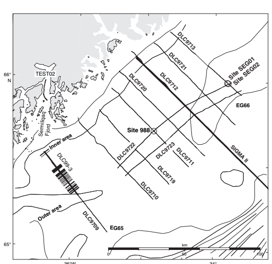

F2. Seismic Line DLC9709, p. 27.

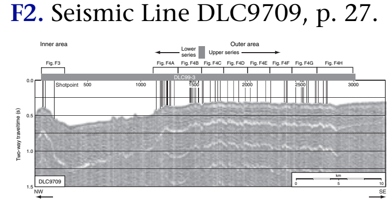

[1]Examples of how to reference the whole or part of this volume.
[2]Scientific Party addresses.

Ms 163XIR-106

sin. This setting is conducive to an offset drilling strategy by providing stratigraphic coverage despite limitations in drilling depth.

PRINCIPAL RESULTS

Drilling on Transect EG65 successfully recovered core at 55 sites over a distance of ~32 km. Forty holes reached volcanic basement. Continental basement (granitic gneiss) was recovered from Hole SEG32A located on the basement high immediately landward of the seismically imaged basin at the northwestern end of Transect EG65 (Fig. F2). In contrast, sites located on the seaward escarpment of this basin recovered friable sandstone (Sites SEG38 and SEG80) and Paleogene lavas, including a distinctive suite of highly to moderately olivine (± plagioclase and clinopyroxene) phyric basalt from Sites SEG77, SEG79, SEG37, SEG75, SEG76, SEG36, SEG74, SEG40, SEG41, SEG42, SEG44, SEG47, and SEG45 (ordered from west to east). Lavas recovered seaward of Site SEG45 are typically aphyric to moderately clinopyroxene-plagioclase phyric. These striking petrographic differences of lavas in the transect area were used to define a lower and upper series, with the boundary placed between Sites SEG45 and SEG51 (~36°17′W) (see Fig. F2).

All igneous units were analyzed by shore-based X-ray fluorescence (XRF). These results show volatiles between 0.5 and 1.5 wt% for most units, whereas the highly olivine phyric flows have volatiles as high as 4 wt%. All of the basalts are olivine and hypersthene normative. A few lavas from the upper series have normative nepheline. The highly to moderately olivine phyric basalts of the lower series have MgO contents as high as 11 wt%, Mg numbers of ~0.68, and TiO_2 contents as low as 0.8 wt%. The basalts are also elevated in Cr and Ni, consistent with their high modal proportion of olivine. In contrast, the plagioclase-clinopyroxene basalts of the upper series have Mg numbers below 0.52 and TiO_2 content reaching 3.8 wt%. Overall, the covariations of major and minor elements are typical of tholeiitic differentiation controlled by olivine, plagioclase, and clinopyroxene fractionation.

The highly to moderately olivine phyric basalts of the lower series commonly have the most calcic plagioclase phenocrysts (An_{87}–An_{76}), Mg-rich clinopyroxene (Mg number = 0.85–0.77), and olivine (Fo_{75}–Fo_{68}) phenocrysts. The sparsely to aphyric upper series reach more evolved phenocryst compositions (plagioclase An_{86}–An_{63}; augite Mg numbers = 0.81–0.71; olivine Fo_{75}–Fo_{61}), despite showing large compositional overlap with the lower series. The most iron-rich olivine (Fo_{54}) was analyzed from the groundmass of Unit I-1 in Hole SEG61B. Spinel is often found in the lower series and is commonly Cr rich (Cr/[Cr + Al + Fe^{3+}] = 0.42–0.59).

All igneous units for which the paleomagnetic polarity could be determined are reversely magnetized. Two samples were deemed suitable for ^{40}Ar-^{39}Ar dating. A plagioclase separate from the upper series (Section 163X-SEG58A-1-1) yields an isochron age of 55.1 ± 0.7 Ma. A whole-rock sample (Section 163X-SEG47A-1-1) of the lower series gives an imprecise isochron age of 51.9 ± 2.3 Ma (C. Tegner, unpubl. data).

The glaciomarine sediments recovered from most of the holes are accumulations of pebble-sized clasts and massive sandy or fine-grained bioturbated diamicton. The contact between the volcanic basement and the overlying glaciomarine sediments was never preserved. Glacial striations and glacially polished surfaces of volcanic basement were recovered from Holes SEG27A and SEG40A, whereas weathering of fractured surfaces is common. These observations suggest that the basement surface was locally barren, glacially eroded, and weathered before being covered by glaciomarine silt and mud containing pebbles and boulders.

The discovery of sandstone at two locations within the lower series is particularly noteworthy. The sandstone recovered from Hole SEG80B is a sulfate-rich, coal flaser–laminated, highly bioturbated, calcite-cemented sandstone containing fossil wood fragments. We interpret this sandstone as a subaqueous deposit formed in the sulfate reduction zone of a calm, shallow basin. A quartzwacke was recovered from Hole SEG38B. Although this material occurs as a 19-cm-long, well-indurated clast, its size, angularity, and the presence of lapilli fragments suggests that it may be Paleogene in age. Furthermore, the presence of rip-up clasts suggests that this unit may have been deposited in a high-energy environment, possibly as fallout from a concentrated turbidite suspension. The structure and age relations of these sediments to the associated lavas are unclear, but it is worth noting the close similarities between the sandstone from Hole SEG80B and sediment recovered from the bottom of ODP Hole 917A, which are stratigraphically below the lower series and interpreted as prebreakup in age (Larsen, Saunders, Clift, et al., 1994), and sediments of the Paleocene Ryberg Formation underlying the Paleogene basalts of the Blosseville Kyst, East Greenland.

GEOPHYSICS AND SITE SELECTION

Approximately 50 preliminary sites for Transect EG65 were selected along seismic Line DLC9709 prior to the leg (Fig. F2). Final site selection was based on sparker seismic Line DLC99-3 shot during the leg. Two separate areas were targeted for drilling:

1. An inner area, including what we believed is a pre-volcanic basin and flanked by basement highs, and
2. An outer area covering the expanse of seaward-dipping reflectors exposed close to the seabed between the inner basin and outer wedge of Eocene–Holocene sediments (Fig. F2).

Sites in the inner area were selected to sample the basin fill and surrounding basement, while those in the outer area targeted as large an age and stratigraphic coverage of the seaward dipping reflectors as possible.

Inner Area

The *Dana* air gun data (seismic Line DLC9709) (Fig. F2) show potential drilling sites near the coast on basement highs and on what is interpreted to be the earliest basin fill. The sparker seismic data (seismic Line DLC99-3) (Fig. F3) indicate that the main part of the basin below the deeper trough further offshore is covered by 5 to 10 m of glacial marine sediment. Potential shallow drill sites were located on highs, in particular, toward the younger and upper part of the basin fill next to the escarpment that separates the basin from the dipping-reflector plateau (Fig. F3). However, drilling in this area mostly failed to recover bedrock below the glacial sediments (Sites SEG32–SEG35). Site SEG32 was successful in recovering continental basement.

F3. Sparker Line DLC99-3, inner area, p. 28.

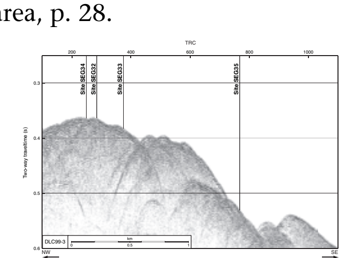

Outer Area

The outer area contains a series of basement highs suitable for drilling (Figs. **F2, F4**). Very little sedimentary fill is seen in the seismic profile between these highs. Where drilling encountered sediment overburden, a clear reflector between the glaciomarine sediment and basement was often lacking. This limited the usefulness of the sparker data and forced the Shipboard Scientific Party to rely heavily on the drillers' judgment of coring conditions. In some instances, basalt was exposed at the seafloor (Fig. **F5**).

F4. Sparker Line DLC99-3, outer area, p. 29.

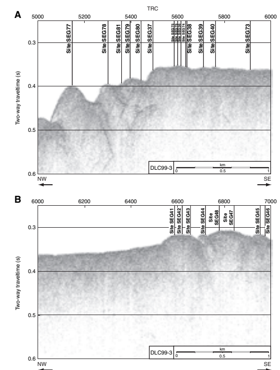

Several holes were attempted within the youngest part of the basin fill next to the escarpment leading up to the seaward-dipping sequence (Fig. **F4A**). The most landward of these sites yielded core of olivine phyric basalt (Site SEG77), unexpected from the features seen in the seismic profiles interpreted to represent small fault blocks with basin fills. Continued drilling attempts eventually recovered micaceous sandstone (Site SEG80) next to the escarpment east of Site SEG77. The volcanic unit recovered at Site SEG77 is interpreted as representing a thin lava cover on top of the basin fill and therefore probably represents some of the very earliest break-up volcanism.

F5. Cold water corals, p. 33.

Drilling closer to the flank of the basin was attempted but had to be abandoned because of dangerous ice conditions. In total, 50 drill sites were located in the outer area.

OPERATIONS

We departed Ammassalik (Greenland) in the early morning of 2 September 1998 in beautiful weather and with all equipment functioning, including the newly installed differential Global Positioning System (DGPS) satellite receiver. Navigational corrections to relate positions and vessel reference points were checked during the port call and the A-frame established as our navigational reference for drilling sites. After collecting seismic sparker Line DLC99-3, we began drilling at Site SEG21. Table **T1** gives a summary of site locations and core recovery.

T1. Core summaries, p. 45.

Drilling operations at Sites SEG21 to SEG24 proceeded without problems; however, at Site SEG25 we began to experience problems with the dynamic positioning controlled by the Trac C navigation system. We experienced more severe problems at Site SEG26 and had to abort drilling at Site SEG27, as the ship's site position could not be maintained. Once these problems were solved, we resumed drilling at Sites SEG28–SEG30 without further incidents. At Site SEG31, the drill rig was accidentally tilted on its side during recovery. The drill crew managed to right the rig without damage to it or the umbilical cable. On the evening of 3 September, increasing sea state and gale winds forced us to seek shelter in the Sermiligaq Fjord. We arrived just before midnight. The weather had improved significantly by morning and we sailed back to the transect area to resume drilling. During the next 2 days we drilled 20 sites (SEG32–SEG52). On four occasions, approaching ice forced us to abandon our position. Site SEG44 had to be abandoned because of a loss of navigational control. On 6 September, during drilling at Site SEG52, a complete failure of the DGPS and loss of the ship's position required an emergency recovery of the drill rig. The rig suffered only slight damage to the bottom of the core barrel. The DGPS was again repaired, and drilling resumed at Sites SEG53–SEG55. While drilling at Site SEG55, an electrical fault caused one of the flush pumps on the drill rig to fail. The drill crew located the fault in the transformer and made a temporary repair, allowing drilling to continue using an auxiliary power cable. Drilling resumed at Site SEG55 on the morning of 7 September and continued at Sites SEG56–SEG66 until 9 September, when damage to the umbilical cable ended the first stage of productive operations. The required repair to the main cable was undertaken during transit in fair weather to Transect EG64.

On 11 September, after finishing our work on Transect EG64, we resumed drilling on Transect EG65. Sites SEG73–SEG81 were drilled, and Site SEG38 was redrilled before increasing wind in the late afternoon of 13 September forced us to pick our way through a corridor of icebergs to again reach shelter in Sermiligaq Fjord. The calm waters in the fjord were used to test an alternative sparker source, collect sparker data along a north–south transect in the fjord (TEST02) (Fig. **F1**), test a camera mounted to the drill rig, and try alternative drill bits. In the early evening of 15 September, we left the shelter of the fjord intending to resume drilling operations off western Iceland, after collecting a total of 25 km of seismic data and drilling 55 sites on Transect EG65. A Force 11+ storm considerably slowed our progress across the Denmark Strait and after 3 days in transit our drilling prospects off Iceland had to be abandoned. Most of the Shipboard Scientific Party disembarked at the port of Keflavik, Iceland, while the remaining crew packed down equipment during the final transit to Leith, Scotland.

SITE SUMMARIES

Brief descriptions of the cores recovered from 90 holes drilled at 55 sites along Transect EG65 are provided below. A summary of the geographical locations of the drilled sites is given in Table **T1.** As for Transect EG68, basement recovery was limited by a cover of glaciomarine sediment of variable thickness containing a high proportion of gravel- to boulder-sized clasts. Despite the difficulties in penetrating this cover, basement was unequivocally sampled in 40 holes.

Site SEG21

Holes SEG21A (Units S-1 and I-1), SEG21AB (Units S-1 and C-1), SEG21AC (Unit S-1), and SEG21AD (Unit I-1)

Four holes were drilled at Site SEG21. Drilling in Hole SEG21A penetrated 0.35 m before coring began, and coring terminated at a depth of 0.51 meters below seafloor (mbsf). Unit S-1 is composed of pebble-sized, angular to subrounded diamicton clasts of weathered basalt. Living barnacles were found attached to one of the clasts. Unit I-1 is 10 cm of sparsely clinopyroxene-plagioclase phyric basalt. Hole SEG21B was drilled immediately after Hole SEG21A without emptying the core barrel. Drilling penetrated 0.38 m before coring began, and coring terminated at 0.44 mbsf. Unit S-1 is diamicton clasts composed of pebble-sized, angular to subrounded clasts of basalt and felsic gneiss. Unit C-1 is 8 cm of moderately clinopyroxene phyric basalt resembling Unit I-1 in Hole SEG21A. Drilling in Hole SEG21C penetrated 0.39 m before coring began, and coring terminated at 0.54 mbsf. Only aphyric basaltic gravel (Unit S-1) was recovered from this hole. Drilling in Hole SEG21D penetrated 0.28 m before coring began, and coring terminated at 0.58 mbsf. Unit I-1 is 31 cm of highly fractured sparsely plagioclase-clinopyroxene-olivine phyric and glomerophyric basalt, based on thin section description. The petrographic similarities between cored basalt recovered from Holes SEG21A, SEG21B, and SEG21D indicate that the volcanic basement was sampled from most holes drilled at Site SEG21.

Site SEG22

Hole SEG22A (Unit I-1)

Drilling in Hole SEG22A penetrated 0.29 m before coring began, and coring terminated at 1.15 mbsf. Unit I-1 is 98 cm of intersertal and moderately plagioclase-clinopyroxene phyric and glomerophyric basalt with 5% plagioclase and traces of clinopyroxene phenocrysts. The volcanic basement was sampled at Site SEG22.

Site SEG23

Hole SEG23A (Unit C-1)

Drilling in Hole SEG23A penetrated 0.50 m before coring began, and coring terminated at 0.72 mbsf. Unit C-1 is composed of cored fragments of fine- to medium-grained, sparsely plagioclase-olivine phyric and glomerophyric basalt. The surfaces of many of the fragments are weathered and suggest that the volcanic basement was not directly sampled at Site SEG23.

Site SEG24

Hole SEG24A (Units S-1 and I-1)

Drilling in Hole SEG24A penetrated 0.40 m before coring began, and coring terminated at 0.90 mbsf. Unit S-1 is a 4-cm subangular clast of sparsely plagioclase-olivine phyric basaltic gravel. Unit I-1 is 53 cm of amygdaloidal, fractured, and moderately plagioclase-clinopyroxene phyric basalt with 5% plagioclase and 2% clinopyroxene phenocrysts. The volcanic basement was sampled at Site SEG24.

Site SEG25

Hole SEG25A (Unit S-1)

Drilling in Hole SEG25A penetrated 0.50 m before coring began, and coring terminated at 1.09 mbsf. Unit S-1 is 15 cm of subangular, pebble-sized, amygdaloidal basaltic clasts with remaining interstitial reddish brown mud. The volcanic basement was not sampled at Site SEG25.

Site SEG26

Hole SEG26A (Unit I-1)

Drilling in Hole SEG26A penetrated 0.30 m before coring began, and coring terminated at 1.39 mbsf. Unit I-1 is 110 cm of moderately plagioclase-clinopyroxene phyric and glomerophyric basalt with 7% plagioclase and 1% clinopyroxene phenocrysts. The unit is extensively fractured. The volcanic basement was sampled at Site SEG26.

Site SEG27

Hole SEG27A (Unit I-1)

Drilling in Hole SEG27A penetrated 0.18 m before coring began, and coring terminated at 1.22 mbsf when the ship lost position. Unit I-1 is 131 cm of highly plagioclase-clinopyroxene-olivine phyric basalt with 10% plagioclase and equal amounts (4%) of clinopyroxene and olivine phenocrysts. The basalt is highly vesicular and amygdaloidal. Live corals were attached to the top surface (Fig. F5), indicating a sediment-free sea bottom. The volcanic basement was sampled at Site SEG27.

Site SEG28

Hole SEG28A (Unit I-1)

Drilling in Hole SEG28A penetrated 0.29 m before coring began, and coring terminated at 0.85 mbsf. Unit I-1 is 48 cm of vesicular, highly plagioclase-olivine-clinopyroxene phyric basalt with 15% plagioclase phenocrysts and minor amounts of clinopyroxene and olivine. The volcanic basement was sampled at Site SEG28.

Site SEG29

Hole SEG29A (Units S-1 and I-1)

Drilling in Hole SEG29A penetrated 1.40 m before coring began, and coring terminated at 2.12 mbsf. Unit S-1 is a 5-cm rounded granite pebble. Unit I-1 is 54 cm of vesicular, moderately plagioclase-olivine-clinopyroxene phyric and glomerophyric basalt with 3% plagioclase and very small amounts of olivine and clinopyroxene phenocrysts. The volcanic basement was sampled at Site SEG29.

Site SEG30

Hole SEG30A (Unit S-1)

Drilling in Hole SEG30A penetrated 0.57 m before coring began, and coring terminated at 1.52 mbsf. Unit S-1 is 23 cm of well-rounded basalt, gneiss, and quartz pebbles. The volcanic basement was not sampled at Site SEG30.

Site SEG31

Hole SEG31A (Unit I-1)

Drilling in Hole SEG31A penetrated 0.66 m before coring began, and coring terminated at 1.36 mbsf. Unit I-1 is 70 cm of vesicular, highly plagioclase-clinopyroxene-olivine phyric and glomerocrystic basalt with 10% plagioclase, 3% clinopyroxene, and 1% olivine phenocrysts. A large 32-cm-long vesicular segregation pipe with sharp but irregular boundaries occurs at the top of the unit (Fig. F6). The volcanic basement was sampled at Site SEG31.

F6. Pipe vesicle, p. 34.

Site SEG32

Holes SEG32A (Unit I-1) and SEG32B (Unit S-1)

Two holes were drilled at Site SEG32. Drilling in Hole SEG32A penetrated 0.80 m before coring began, and coring terminated at 1.32 mbsf. Unit I-1 is 23 cm of melanocratic hornblende-biotite pegmatite with interstitial oxides believed to represent the Archean basement. The gneiss is composed of hornblende, biotite, quartz, and opaque minerals. Drilling in Hole SEG32B penetrated 0.82 m before coring began, and coring terminated at 1.82 mbsf. Unit S-1 is 23 cm of diamicton clasts including basalt and quartzite. The continental basement was sampled at Site SEG32.

Sites SEG33 and SEG34

Holes SEG33A and SEG34A (no recovery)

Drilling in Holes SEG33A and SEG34A penetrated to depths of 2.09 and 0.68 mbsf, respectively. No core was recovered from these holes.

Site SEG35

Hole SEG35A (Unit S-1)

Drilling in Hole SEG35A penetrated 1.88 m before coring began, and coring terminated at 3.00 mbsf. Unit S-1 is three subangular to rounded pebbles of basaltic to arkosic rock fragments. The volcanic basement was not sampled at Site SEG35.

Site SEG36

Hole SEG36A (Unit I-1)

Drilling in Hole SEG36A penetrated 0.60 m before coring began, and coring terminated at 0.86 mbsf. Unit I-1 is 25 cm of highly amygdaloidal, moderately olivine-clinopyroxene-plagioclase phyric olivine basalt, with 5% olivine, 3% clinopyroxene, and small amounts of plagioclase phenocrysts. Spherical vesicles are filled with chlorite, albite, and calcite. The groundmass is highly silicified and olivine phenocrysts are completely altered to rusty red iddingsite. This unit is distinctive in terms of both its general appearance and its original phenocryst assemblage of olivine and clinopyroxene. We conclude that the volcanic basement was sampled at Site SEG36.

Site SEG37

Hole SEG37A (Unit C-1)

Drilling in Hole SEG37A penetrated 1.40 m before coring began, and coring terminated at 3.00 mbsf. Unit C-1 is a 7-cm-long cored clast of aphyric basalt, relatively similar to Unit I-1 in Hole SEG36A. Because of the petrographic similarity to Unit I-1 in Hole SEG36A, it is suggested that Unit C-1 represents a locally derived block of the volcanic basement.

Site SEG38

Holes SEG38A (no recovery), SEG38B (Unit S-1), and SEG38C (Unit S-1)

Three holes were drilled at Site SEG38. The attempt to drill Hole SEG38A was terminated by an approaching ice flow and no recovery was made. Drilling in Hole SEG38B penetrated 0.91 m before coring began, and coring terminated at 1.88 mbsf. Unit S-1 is 32 cm of diamicton clasts of very variable compositions and sizes, including coarse-grained amphibolites and a 19-cm-long fragment of gray sandstone. The latter consists of subangular and cemented fragments of quartz, mica, feldspar, epidote, and carbon flasers cemented by calcite. Drilling in Hole SEG38C penetrated 1.28 m before coring began, and coring terminated at 1.85 mbsf. Unit S-1 is 7 cm of olivine phyric and aphyric basaltic pebbles. The volcanic basement was not sampled at Site SEG38.

Site SEG39

Hole SEG39A (Unit S-1)

Drilling in Hole SEG39A penetrated 0.60 m before coring began, and coring terminated at 1.19 mbsf. Unit S-1 is 12 cm of subangular to rounded clasts of basalt and sandstone. Some clasts show glacial striations. The volcanic basement was not sampled at Site SEG39.

Site SEG40

Hole SEG40A (Unit I-1)

Drilling in Hole SEG40A penetrated 0.65 m before coring began, and coring terminated at 1.89 mbsf. Unit I-1 is 118 cm of highly olivine phyric olivine basalt. Glacial striations occur on the top surface of Unit I-1. Olivine phenocrysts are completely altered to iddingsite and lizardite. Plagioclase glomerocrysts are recognized in thin section. Amygdules are filled with calcite, chlorite, and quartz. This unit has the distinctive appearance first noted in Unit I-1 at Site SEG36. We conclude that the volcanic basement was sampled at Site SEG40.

Site SEG41

Hole SEG41A (Unit I-1)

Drilling in Hole SEG41A started coring when the drill touched the seafloor, and coring terminated at a depth of 0.42 mbsf. Unit I-1 is 23 cm of amygdaloidal, highly plagioclase-olivine-clinopyroxene phyric olivine basalt with most phenocrysts in glomerocrysts and 8% plagioclase, 2% olivine, and small amounts of clinopyroxene phenocrysts. Live corals and other life forms were found on top pieces and demonstrate the lack of sediment cover at this site. This unit resembles Unit I-1 at Site SEG36. The volcanic basement was sampled at Site SEG41.

Site SEG42

Holes SEG42A (Unit C-1), SEG42B (Unit I-1), and SEG42C (Units S-1 and I-1)

Three holes were drilled at Site SEG42. Drilling in Hole SEG42A penetrated 0.58 m before coring began, and coring terminated at 1.14 mbsf. Unit C-1 is 15 cm of fresh, amygdaloidal, highly olivine-clinopyroxene phyric basalt clasts. Drilling in Hole SEG42B penetrated 0.95 m before coring began, and coring terminated at 1.40 mbsf. Unit I-1 is 40 cm of seriate and amygdaloidal, highly olivine -plagioclase phyric basalt with 12% olivine and 10% plagioclase phenocrysts. Vesicles are lined successively with chlorite, quartz, and calcite. The groundmass is highly silicified, and olivine phenocrysts are completely altered to iddingsite. Drilling in Hole SEG42C penetrated 1.39 m before coring began, and coring terminated at 1.91 mbsf. Unit S-1 is 8 cm of mainly basaltic pebbles. Unit I-1 is 40 cm of vesicular and amygdaloidal, highly plagioclase-olivine-clinopyroxene phyric basalt with 7% plagioclase, 6% olivine, and 3% clinopyroxene phenocrysts. The highly olivine-plagioclase phyric units recovered from all holes at Site SEG42 are petrographically similar to the volcanic units first observed at Site SEG36. The volcanic basement was sampled at Site SEG42.

Site SEG43

Hole SEG43A (Unit I-1)

Drilling in Hole SEG43A penetrated 0.62 m before coring began, and coring terminated at 1.12 mbsf. Unit I-1 is 47 cm of vesicular and highly olivine-plagioclase-clinopyroxene phyric basalt with 10% olivine, 9% plagioclase, and 2% clinopyroxene phenocrysts, similar to the volcanic units first observed at Site SEG36. The volcanic basement was sampled at Site SEG43.

Site SEG44

Hole SEG44A (Unit I-1)

Drilling in Hole SEG44A penetrated 0.26 m before coring began, and coring terminated at 0.72 mbsf. Unit I-1 is 46 cm of vesicular, banded, and sparsely olivine phyric olivine basalt. This unit is petrographically similar to the volcanic units first observed at Site SEG36. The volcanic basement was sampled at Site SEG44.

Site SEG45

Hole SEG45A (Units S-1 and I-1)

Drilling in Hole SEG45A penetrated 0.48 m before coring began, and coring terminated at 1.12 mbsf. Unit S-1 is 16 cm of diamicton clasts composed of subangular to rounded pebbles of basalt, gneiss, and granite. Unit I-1 is 33 cm of moderately olivine-clinopyroxene-plagioclase phyric and highly amygdaloidal basalt with 4% olivine, 4% clinopyroxene, and 2% plagioclase phenocrysts. It is very highly altered and fractured with a crumbling appearance. This unit is petrographically similar to the volcanic units first observed at Site SEG36. The volcanic basement was sampled at Site SEG45.

Site SEG46

Hole SEG46A (Unit S-1)

Drilling in Hole SEG46A penetrated 0.82 m before coring began, and coring terminated at 0.92 mbsf. Unit S-1 is 22 cm of mostly basaltic pebbles, although some gneiss and granite pebbles are present as well. The volcanic basement was not sampled at Site SEG46.

Site SEG47

Hole SEG47A (Units S-1 and I-1)

Drilling in Hole SEG47A penetrated 0.52 m before coring began, and coring terminated at 0.96 mbsf. Unit S-1 is 16 cm of angular to subrounded basaltic and gneissic pebbles. Unit I-1 is 58 cm of fresh, amygdaloidal, sparsely olivine-clinopyroxene phyric basalt. This unit is petrographically similar to the volcanic units first observed at Site SEG36. The volcanic basement was sampled at Site SEG47.

Site SEG48

Hole SEG48A (Unit S-1)

Drilling in Hole SEG48A penetrated 1.90 m before coring began, and coring terminated at 2.11 mbsf. Unit S-1 is 71 cm of diamicton composed of matrix supported muddy sandstone with foraminifers. The sandstone is matrix-supported and poorly sorted with rounded diverse clasts, including ~8% basaltic and other rock fragments. The volcanic basement was not sampled at Site SEG48.

Site SEG49

Hole SEG49A (Unit S-1)

Drilling in Hole SEG49A penetrated 0.79 m before coring began, and coring terminated at 1.46 mbsf. Unit S-1 is 50 cm of diamicton composed of matrix-supported, poorly sorted muddy sandstone with foraminifers and a gravel layer with pebble-sized, subrounded basaltic and gneissic clasts. Unit S-1 is very similar to Unit S-1 in Hole SEG48A. The volcanic basement was not sampled at Site SEG49.

Site SEG50

Hole SEG50A (Unit S-1)

Drilling in Hole SEG50A penetrated 1.66 m before coring began, and coring terminated at 1.77 mbsf. Unit S-1 is 33 cm of diamicton composed of an accumulation of mostly basaltic, pebble-sized, angular to subrounded clasts. The volcanic basement was not sampled at Site SEG50.

Site SEG51

Holes SEG51A (Unit I-1), SEG51B (Unit I-1), and SEG51C (Units S-1, I-1)

Drilling in Hole SEG51A penetrated 0.42 m before coring began, and coring terminated at 0.59 mbsf. Unit I-1 is 52 cm of amygdaloidal, highly fractured, moderately plagioclase-clinopyroxene phyric basalt. This unit may represent flow top rubble. Drilling in Hole SEG51B penetrated 0.41 m before coring began, and coring terminated at 0.56 mbsf. Unit I-1 is 23 cm of moderately olivine-clinopyroxene phyric olivine-basalt with 3% olivine and 2% clinopyroxene phenocrysts. A 1-cm-sized xenolith of olivine and pyroxene was discovered after splitting the core. Drilling in Hole SEG51C penetrated 0.44 m before coring began, and coring terminated at 0.92 mbsf. Unit S-1 is a 22-cm accumulation of mostly basaltic pebble-sized clasts that also include a small foliated gneissic clast. Unit I-1 is 23 cm of vesicular, moderately clinopyroxene-plagioclase phyric basalt with 5% clinopyroxene and 3% plagioclase phenocrysts. It is brecciated, cemented with quartz and calcite, and resembles a flow top. The volcanic basement was sampled at Site SEG51.

Site SEG52

Hole SEG52A (Units S-1 and I-1)

Drilling in Hole SEG52A penetrated 0.28 m before coring began, and coring terminated at 0.46 mbsf. Unit S-1 is a 10-cm accumulation of pebble-sized rock fragments including basaltic and gneissic varieties. Unit I-1 is 21 cm of sparsely plagioclase-clinopyroxene phyric and glomerophyric basalt with oxidized fractures. The volcanic basement was sampled at Site SEG52.

Site SEG53

Holes SEG53A (Unit I-1) and SEG53B (Unit I-1)

Drilling in Hole SEG53A penetrated 0.37 m before coring began, and coring terminated at 0.60 mbsf because of an approaching iceberg. Unit I-1 is 22 cm of amygdaloidal and aphyric basalt. Drilling in Hole SEG53B penetrated 0.36 m before coring began, and coring terminated at 0.72 mbsf. Unit I-1 is 31 cm of amygdaloidal, aphyric basalt that is similar to Unit I-1 of Hole SEG53A. The basalts in both holes are highly altered and fractured and appear angular and subrounded in the core. Because all pieces are petrographically very similar, both units were classified as igneous. The volcanic basement was sampled at Site SEG53.

Site SEG54

Hole SEG54A (Units S-1 and I-1)

Drilling in Hole SEG54A penetrated 0.44 m before coring began, and coring terminated at 0.71 mbsf. Unit S-1 is 3 cm of subrounded basaltic pebbles. Unit I-1 is 19 cm of sparsely clinopyroxene-plagioclase-olivine phyric basaltic clasts with 5% clinopyroxene, 2% plagioclase, and 1% olivine phenocrysts. The petrography of Unit I-1 is similar to igneous units in Holes SEG52A, SEG53A, and SEG53B and suggests that the volcanic basement was sampled at Site SEG54. Unit I-1 was classified as an igneous unit despite the lowermost clast in the section being subrounded with weathered, fractured surfaces.

Site SEG55

Holes SEG55A (no recovery), SEG55B (Units S-1 and I-1), and SEG55C (Units S-1 and C-1)

Drilling in Hole SEG55A made no recovery. Drilling in Hole SEG55B penetrated 0.60 m before coring began, and coring terminated at 0.98 mbsf. Unit S-1 is 12 cm of subangular to subrounded pebbles of basaltic, dioritic, and granitic compositions, some with small amounts of adhering mud. Unit I-1 is 20 cm of vesicular and sparsely plagioclase phyric basalt. Drilling in Hole SEG55C penetrated 0.15 m before coring began, and coring terminated at 0.32 mbsf. Unit S-1 is 4 cm of subangular, pebble-sized clasts of basalt and diorite. Unit C-1 is 9 cm of cored basalt clasts consisting of amygdaloidal, moderately plagioclase-clinopyroxene-olivine phyric and glomerophyric basalts. Small inclusions are millimeter sized and fresh and contain olivine and pyroxene. Unit C-1 is very similar to Unit I-1 in Hole SEG55B and is interpreted to be a locally derived basaltic clast. It is concluded that the volcanic basement was sampled at both Holes SEG55B and SEG55C.

Site SEG56

Holes SEG56A (Units S-1 and I-1) and SEG56B (Units S-1 and C-1)

Two holes were drilled at Site SEG56. Drilling in Hole SEG56A penetrated 0.30 m before coring began, and coring terminated at 0.71 mbsf. Unit S-1 is 7 cm of diamicton clasts composed of subangular pebbles of basaltic, dioritic, and biotite granitic rocks. Unit I-1 is 28 cm of amygdaloidal, highly plagioclase-olivine-clinopyroxene phyric and glomerophyric olivine basalt with 6% plagioclase, 4% clinopyroxene, and 2% olivine phenocrysts and a trachytic groundmass texture. Drilling in Hole SEG56B penetrated 0.37 m before coring began, and coring terminated at 0.60 mbsf. Unit S-1 is a single subangular pebble of biotite felsic gneiss. Unit C-1 is 14 cm of cored and rounded clasts of amygdaloidal, moderately plagioclase-olivine-clinopyroxene phyric to glomerophyric basalt with trachytic alignment of plagioclase laths in the groundmass. The two basalt units defined at this site are petrographically very similar. The units are also similar to Unit I-1 in Hole SEG57A and probably represent the local volcanic basement.

Site SEG57

Hole SEG57A (Unit I-1)

Drilling in Hole SEG57A penetrated 0.48 m before coring began, and coring terminated at 0.87 mbsf. Unit I-1 is 45 cm of amygdaloidal, moderately plagioclase-olivine-clinopyroxene phyric basalt with 2% plagioclase, 2% olivine, and 1% clinopyroxene phenocrysts. The basalt has a trachytic groundmass. The unit is petrographically very similar to Unit C-1 in Hole SEG56B. The volcanic basement was sampled at Site SEG57.

Site SEG58

Hole SEG58A (Unit I-1)

Drilling in Hole SEG58A penetrated 0.57 m before coring began, and coring terminated at 1.13 mbsf. Unit I-1 is 27 cm of seriate, highly plagioclase-olivine-clinopyroxene phyric and glomerophyric basalt with 8% plagioclase, 4% olivine, and 2% clinopyroxene phenocrysts. The volcanic basement was sampled at Site SEG58.

Site SEG59

Holes SEG59A (Unit C-1) and SEG59B (Unit S-1)

Both holes drilled at Site SEG59 sampled a thin sediment cover without reaching the volcanic basement. Drilling in Hole SEG59A penetrated 0.40 m before coring began, and coring terminated at 0.80 mbsf. Unit C-1 is 16 cm of subangular, sparsely clinopyroxene-plagioclase phyric basaltic clasts and gneissic clasts. Drilling in Hole SEG59B penetrated 0.32 m before coring began, and coring terminated at 0.32 mbsf. Unit S-1 is 16 cm of sparsely clinopyroxene-plagioclase phyric basaltic and granitic clasts. The volcanic basement was not sampled at Site SEG59.

Site SEG60

Holes SEG60A (Unit C-1) and SEG60B (Unit I-1)

Drilling in Hole SEG60A penetrated 0.42 m before coring began, and coring terminated at 0.51 mbsf. Unit C-1 is a 3 cm highly plagioclase-olivine phyric basaltic clast. Drilling in Hole SEG60B penetrated 0.35 m before coring began, and coring terminated at 1.35 mbsf. Unit I-1 is 103 cm of amygdaloidal, moderately plagioclase-olivine-clinopyroxene phyric and intersertal basalt with 5% plagioclase, 4% olivine, and 1% clinopyroxene phenocrysts. The uppermost part of Unit I-1 is very vesicular and fractured and may represent a flow top. The volcanic basement was sampled at Site SEG60.

Site SEG61

Holes SEG61A (Units S-1 and I-1) and SEG61B (Unit I-1)

Drilling in Hole SEG61A penetrated 0.36 m before coring began, and coring terminated at 0.82 mbsf. Unit S-1 is a 13-cm-long foliated gneissic clast with various forms of benthic organisms growing on the top weathered surface. Unit I-1 is 62 cm of vesicular, moderately clinopyroxene-olivine phyric basalt. Drilling in Hole SEG61B penetrated 0.30 m before coring began, and coring terminated at 1.67. Unit I-1 is 156 cm of moderately plagioclase-clinopyroxene-olivine phyric basalt with 5% plagioclase, 1% clinopyroxene, and 1% olivine phenocrysts. The volcanic basement was sampled at Site SEG61.

Site SEG62

Hole SEG62A (Units S-1 and I-1)

Drilling in Hole SEG62A penetrated 0.42 m before coring began, and coring terminated at 0.94 mbsf. Unit S-1 is 9 cm of subangular basaltic pebbles. Unit I-1 is 30 cm of vesicular, moderately plagioclase-clinopyroxene phyric basalt with 5% plagioclase and 2% clinopyroxene phenocrysts. The volcanic basement was sampled at Site SEG62.

Site SEG63

Holes SEG63A (Unit I-1) and SEG63B (Unit I-1)

Drilling in Hole SEG63A penetrated 0.80 m before coring began, and coring terminated at 1.01 mbsf. Unit I-1 is 30 cm of vesicular to glomerophyric, moderately plagioclase-olivine-clinopyroxene phyric basalt with rusty-brown weathering and contains 2% plagioclase, 1% olivine, and 1% clinopyroxene phenocrysts. Drilling in Hole SEG63B penetrated 0.48 m before coring began, and coring terminated at 0.91 mbsf. Unit I-1 is 55 cm of basalt very similar to basalt recovered from Unit I-1 in Hole SEG63A. These petrographic similarities suggest that Unit I-1 in Hole SEG63A may represent the local volcanic basement similar to basement sampled by Unit I-1 in Hole SEG63B. The volcanic basement was sampled at Site SEG63.

Site SEG64

Holes SEG64A (Unit S-1) and SEG64B (Unit C-1)

Drilling in Hole SEG64A penetrated 0.48 m before coring began, and coring terminated at 0.65 mbsf. Unit S-1 is 17 cm of subangular to rounded clasts consisting of basalt, granite, and sandstone. Drilling in Hole SEG64B penetrated 0.30 m before coring began, and coring terminated at 0.87 mbsf. Unit C-1 is an 8-cm-long core of a moderately plagioclase-clinopyroxene phyric basaltic boulder with a weathered and rounded lower surface. The volcanic basement was not sampled at Site SEG64.

Site SEG65

Holes SEG65A (Units S-1 and I-1) and SEG65B (Units S-1 and I-1)

Drilling in Hole SEG65A penetrated 0.40 m before coring began, and coring terminated at 0.68 mbsf. Unit S-1 is 4 cm long and composed of two pebble-sized clasts of granite and basalt. Unit I-1 is 27 cm of amygdaloidal, moderately olivine-clinopyroxene-plagioclase phyric basalt with 5% olivine, 3% clinopyroxene, and 2% olivine phenocrysts. Drilling in Hole SEG65B penetrated 0.25 m before coring began, and coring terminated at 0.57 mbsf. Unit S-1 is 4 cm of small, pebble-sized basaltic and gneissic clasts and a ~2.5-cm-long unspecified snail shell. Unit I-1 is 26 cm of moderately olivine-clinopyroxene-plagioclase phyric and glomerophyric basalt. The volcanic basement was sampled at Site SEG65.

Site SEG66

Hole SEG66A (Unit S-1)

Drilling in Hole SEG66A penetrated 0.30 m before coring began, and coring terminated at 0.60 mbsf. Unit S-1 is 16 cm of subangular, moderately, plagioclase-clinopyroxene phyric basaltic pebbles of nearly identical petrographic characteristics. The volcanic basement was not sampled at Site SEG66.

Site SEG73

Holes SEG73A (no recovery) and SEG73B (Unit S-1)

The attempt to drill Hole SEG73A terminated at 1.13 mbsf when the ship lost positioning. Drilling in Hole SEG73B stepped rapidly to a full penetration depth of 3.00 mbsf. Unit S-1 is 14 cm of rounded to subangular diamicton clasts with basaltic and gneissic compositions. The volcanic basement was not sampled at SEG73.

Site SEG74

Holes SEG74A (Units S-1 and I-1), SEG74B (Unit S-1), SEG74C (no recovery), SEG74D (Unit S-1), and SEG74E (Units S-1 and C-1)

Drilling in Hole SEG74A penetrated 1.60 m before coring began, and coring terminated at 1.93 mbsf. Unit S-1 is 4 cm of sparsely plagioclase-clinopyroxene phyric basaltic gravel. Unit I-1 is 27 cm of massive, nonvesicular, highly olivine phyric basalt with strong orange coloration from weathering. Almost all phenocrysts are altered to red clay. Fractures occur frequently and are filled by red alteration clay and occasionally lined by a black mineral. This unit is petrographically similar to the distinctive volcanic units first observed at Site SEG36. Drilling in Hole SEG74B penetrated 1.10 m before coring began, and coring terminated at 1.20 mbsf. Unit S-1 contains subangular to subrounded pebbles with a range of compositions including basalt, gneiss, and metamorphic quartzite. Two clasts have a composition similar to Unit I-1 in Hole SEG74A. Hole SEG74C was drilled 15 m northwest offset from the original target. Drilling penetrated 0.43 m before coring began, and coring terminated at 0.51 mbsf without core recovery. Hole SEG74D was drilled at the same location as Hole SEG74C. Drilling penetrated 0.71 m before coring began, and coring terminated at 1.01 mbsf. Unit S-1 is 17 cm long and composed of 2- to 4-cm-sized pebbles of basalt and sandstone. The sandstone consists mainly of quartz and mica. The basaltic pebbles are highly weathered, red-stained, and moderately olivine phyric (~10% olivine). Olivine phenocrysts are ~2 mm in diameter, and all are altered to a green mineral and iddingsite. Amygdules are ~1 mm in diameter, ellipsoidal, and filled with green minerals that have red stains around the rims. The basaltic pebbles are similar to Unit I-1 in Hole SEG74A. Hole SEG74E was drilled at the same location as Holes SEG74C and SEG74D and penetrated 0.87 m before coring began. Coring terminated at 2.4 mbsf. Unit S-1 is composed of <1-cm-sized basaltic gravel with a composition similar to that of Unit I-1 in Hole SEG74A. Unit C-1 is a 7-cm-long cored clast of moderately plagioclase-olivine-clinopyroxene phyric basalt with 5% plagioclase, 2% olivine, and 1% clinopyroxene phenocrysts. Plagioclase and clinopyroxene form glomerocrysts, with olivine occasionally composing part of the glomerocrystic assemblage. Vesicles are ~0.5–2 mm in diameter and most commonly unfilled, although some have white zeolite fillings. Small vesicles occur in irregular swarms. Unit C-1 is different from Unit I-1 in Hole SEG74A. The volcanic basement was sampled at Site SEG74.

Site SEG75

Holes SEG75A (Units S-1 and C-1), SEG75B (Units S-1 and I-1), and SEG75C (Units S-1, S-2, and I-1)

Drilling in Hole SEG75A penetrated 1.68 m before coring began, and coring terminated at 1.94 mbsf. Unit S-1 is 22 cm of basaltic gravel consisting of highly olivine-clinopyroxene phyric basalt similar to the underlying Unit C-1. Unit C-1 is a 4-cm-long cored clast of highly olivine-clinopyroxene phyric (10% olivine and 1% clinopyroxene), amygdaloidal, very highly altered basalt. All olivine phenocrysts have been replaced by green clays and iddingsite. Amygdules are most often lined with a dark green mineral, possibly epidote, and filled with clays, carbonate, and zeolites. The high content of amygdules indicate that Unit C-1 represents a pahoehoe flow top. Drilling in Hole SEG75B penetrated 1.68 m before coring began, and coring terminated at 1.93 mbsf. Unit S-1 is a 3-cm-long clast of moderately olivine phyric basalt, different in composition from the underlying Unit I-1. Unit I-1 is 27 cm of amygdaloidal, highly olivine-clinopyroxene phyric (10% olivine and 1% clinopyroxene), very highly altered basalt. All olivine phenocrysts are altered to green clays and iddingsite. Amygdules are most often lined with a dark green mineral, possibly epidote, and filled with pale green to white clays, carbonate, and zeolites. Drilling in Hole SEG75C penetrated 1.40 m before coring began, and coring terminated at 1.92 mbsf. Unit S-1 is 3 cm of basaltic gravel with a composition similar to Unit S-1 in Hole SEG75B. Unit S-2 is 24 cm of highly olivine-clinopyroxene phyric basaltic gravel similar to the underlying Unit I-1. Unit I-1 is 18 cm of fine-grained, amygdaloidal, highly olivine-clinopyroxene phyric basalt (10% olivine and 1% clinopyroxene). The basalt is very highly altered and with vesicles filled by green clay minerals. This unit is petrographically similar to the distinctive volcanic units first observed at Site SEG36. Unit I-1 is petrographically similar to clasts in Units S-1 and C-1 of Hole SEG75A. The volcanic basement was sampled at SEG75.

Site SEG76

Holes SEG76A (Units S-1 and C-1) and SEG76B (Units S-1 and C-1)

Drilling in Hole SEG76A penetrated 0.30 m before coring began, and coring terminated at 0.41 mbsf. Unit S-1 is a 3-cm subangular diamicton clast of gneissic composition. Unit C-1 is an 8-cm-long clast of aphyric basalt. The basalt is very highly altered with a yellowish brown appearance and is amygdaloidal with 0.5- to 2-mm spherically to irregularly shaped amygdules filled with orange and red clay minerals. Drilling in Hole SEG76B penetrated 1.12 m before coring began, and coring terminated at 1.40 mbsf. Unit S-1 is 10 cm of diamicton clasts consisting of subangular to subrounded clasts of gneiss and sandstone.

Unit C-1 is 11 cm of cored clasts of fine-grained, highly olivine phyric basaltic composition with 50% olivine phenocrysts. The basalt is nonvesicular and apparently very fresh but different from the clast in Hole SEG76A. Unit C-1 is petrographically similar to the distinctive olivine phyric igneous units first recovered from Site SEG36. The volcanic basement may have been sampled at SEG76.

Site SEG77

Holes SEG77A (Units S-1 and I-1), SEG77B (Subunits S-1a and S-1b), and SEG77C (Unit S-1)

Drilling in Hole SEG77A penetrated 0.66 m before coring began, and coring terminated at 1.07 mbsf. Unit S-1 is 8 cm of moderately olivine phyric basaltic clasts compositionally similar to the underlying unit. Unit I-1 is 43 cm of fine-grained, amygdaloidal and vesicular, moderately olivine phyric basalt that is highly altered with 4% olivine phenocrysts. Large (0.5–4 mm) round to very elongate vesicles are filled with dark brown to yellow clays. Some vesicles are elongated in the same direction, which may be a flow feature. This unit is petrographically similar to the distinctive olivine phyric igneous and clast units first recovered from Site SEG36. Drilling in Hole SEG77B penetrated 0.40 cm before coring began, and coring terminated at 0.60 mbsf. Subunit S-1a is a 2-cm-long gneissic clast. Subunit S-1b is 36 cm of moderately olivine-phyric basaltic gravel similar to Unit I-1 in Hole SEG77A. Hole SEG77C was relocated ~10 m southeast of the original site target and drilling penetrated 0.56 m before coring began. Coring terminated at 1.47 mbsf. Unit S-1 is 49 cm of moderately olivine phyric basaltic gravel compositionally similar to Unit I-1 in Hole SEG77A. The volcanic basement was sampled at SEG77.

Site SEG78

Hole SEG78A (no recovery)

It was not possible to find stable ground for the drill rig on the seabed. No material was recovered from Hole SEG78A.

Site SEG79

Holes SEG79A (no recovery), SEG79B (no recovery), and SEG79C (Subunits S-1a and S-1b and Unit C-1)

Drilling in Hole SEG79A penetrated 0.56 m before coring began, and coring terminated at 0.82 mbsf without recovery. Drilling in Hole SEG79B penetrated 0.32 m before coring began but terminated without recovery because of approaching ice flows. Hole SEG79C was drilled at a location offset ~10 m southeast from the original site target. Drilling penetrated 0.52 m before coring began, and coring terminated at 0.68 mbsf. Subunit S-1a is 2 cm of aphyric, fine-grained, reddish brown basaltic gravel. Subunit S-1b is 17 cm of highly olivine phyric basalt gravel similar to the underlying Unit C-1. Unit C-1 is a 16-cm-long cored clast of massive, highly olivine phyric basalt with a possibly glacially polished upper surface. The basalt contains 12% olivine and ~1% clinopyroxene and is moderately altered. Unit C-1 is petrographically similar to the distinctive olivine phyric igneous and clast units first recovered at Site SEG36. The volcanic basement may have been sampled at SEG79.

Site SEG80

Holes SEG80A (Units S-1 and C-1) and SEG80B (Unit S-1 and S-2)

Drilling in Hole SEG80A was erratic, and coring terminated at 1.88 mbsf. Unit S-1 is 2 cm of diamicton clasts of basaltic and hornblende-biotite-garnet gneissic compositions. Unit C-1 is composed of medium-grained, porphyritic, highly clinopyroxene-plagioclase-olivine phyric basaltic clast that is moderately altered. Drilling in Hole SEG80B penetrated 2.54 m before coring began, and coring terminated at 3.00 mbsf. Unit S-1 is 3 cm of diamicton clasts of subrounded basalt and gneissic pebbles. Unit S-2 is 61 cm of gray, highly bioturbated, calcite-cemented but fragile micaceous sandstone with coal flasers (Fig. F7). Unit S-2 is interpreted to represent in situ sampling of the prebasaltic basin fill. The volcanic basement was not sampled at SEG80.

F7. Friable sandstone, p. 35.

Site SEG81

Holes SEG81A (Unit S-1) and SEG81B (no recovery)

Drilling in Hole SEG81A terminated at 1.88 mbsf. Unit S-1 is 11 cm of diamicton clasts composed of 2- to 3-cm, large subangular fragments of sandstone and gneiss. Drilling in Hole SEG81B penetrated to 1.36 m and then stepped to 1.89 mbsf, where drilling was terminated without recovery. The volcanic basement was not sampled at Site SEG81.

SEDIMENTARY PETROLOGY

The glacial sedimentary units recovered from Transect EG65 are very similar to those recovered from Transect EG68. The cored glacial sediments are divided into three facies: (1) pebble-sized clasts, (2) massive sandy diamicton, and (3) fine-grained diamicton with bioturbation. The sandy fraction in Unit S-1 of Hole SEG48A is composed of angular fragments of quartz, alkali feldspar, amphibole, basaltic lapilli, and shell fragments (Fig. F8).

F8. Sand-size fraction, p. 36.

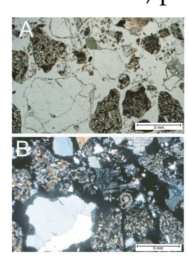

Preglacial sediments recovered from two sites are particularly interesting. A gray, fine-grained, well-indurated quartzwacke unit (S-1) with rip-up clasts was recovered from Hole SEG38B (Sample 163X-SEG38B-1-1 [Piece 2, 8–27 cm]) (Fig. F9). The rip-up clasts are randomly oriented with irregular, rounded dish shapes. The unit is moderately sorted with grains ranging from clay to medium-sand size cemented by calcite. In thin section, the unit has an isotropic clast fabric of subrounded, low sphericity quartz (50%); clay (8%); subangular to angular grains of calcite (8%), muscovite (1%), and epidote (1%); and carbon flakes (3%). The poorly sorted, random distribution of the irregularly shaped rip-up clasts and high clay and carbon content of this unit suggest deposition under high-energy conditions, possibly as fall-out from a sediment load of a highly concentrated turbidite current suspension. Such a depositional environment, however, is difficult to reconcile with an in situ position between subaerially erupted lavas; therefore the unit might be a glacial clast.

F9. Consolidated quartzwacke, p. 37.

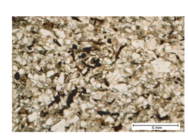

Unit S-2 in Hole SEG80B is a bioturbated, poorly indurated, gray micaceous sandstone with coal flasers (Figs. F7). The fine-grained (silt to medium grained) sandstone is generally well sorted with a porosity value of ~30%. The original planar and small-scale cross-lamination is disturbed by 5- to 30-mm-long, 2–4 mm in diameter vertical and subhorizontal burrows. Coal flasers are abundant as discontinuous drapings with alignment of minute fragments parallel to the bedding. The best examples of coal flasers are found between 19.3 and 30.0 cm in Section 163X-SEG80B-1-1. A fossil wood fragment as large as 2 cm in diameter occurs 35 cm below the top of Unit S-2. The coal has generally high vitrinite reflectance.

In thin section the sediment is dominated by angular grains of quartz with high sphericity (>60%) and feldspar, giving the sandstone an arkosic composition (Fig. F10). Subordinate amounts of muscovite and hornblende and trace amounts of pyrite occur. The heavy mineral assemblage is dominated by zircons. Pyrite is the first authigene phase and is closely connected to organic debris, which is mainly plant fragments. The pyrite is followed by Ti oxides, probably anatase, precipitated in the close vicinity of dissolved titanoferous grains. These authigene phases were cemented by the widespread development of alkali feldspar overgrowths on detrital, dominantly angular feldspar grains. The sparse amount of quartz overgrowths developed contemporary with the prevalent authigene alkali feldspars. After these early diagenetic phases, the sandstone experienced incipient mechanical compaction, as evidenced by slightly bent mica grains and minor grain crushing. Sporadic calcite cementation occurred in the open framework, replacing some of the detrital feldspar grains and occluding porosity locally (Fig. F10). The last diagenetic episode was an intense dissolution of feldspar grains that resulted in high amounts of secondary porosity. The dissolution phase seems selective; preferably dissolving detrital feldspar grains compared to detrital and authigenic alkali feldspar. Dissolution does not seem to have affected calcite, and preferable feldspar dissolution inside calcite cemented areas is widespread. The skeletal grain remnants are not affected by later compaction (Fig. F10), though the authigene cements were only able to stabilize the grain framework in limited amount. Therefore, the sandstone does not seem to have experienced high mechanical compaction and deep burial.

F10. Fine-grained arkosic sandstone, p. 38.

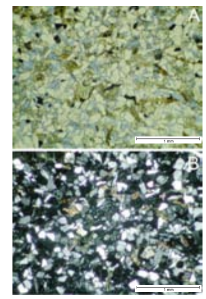

Two samples from Unit S-2 were processed for palynological examination at the Geological Survey of Denmark and Greenland (GEUS). The samples are dominated by tracheids and black coal particles; however, dinoflagellate cysts were recovered from both samples. The dinoflagellate cysts are well preserved and only slightly affected by thermal heating during burial. The density and diversity is low. The dominant species are *Oligosphaeridium* sp. 1 Nøhr-Hansen 1993 and *Circulodinium* sp. 1 Nøhr-Hansen 1993, together with a few specimens of *Circulodinium distinctum, Leptodinium cancellatum, Microdinium dentatum, Odontochitina operculata, Oligosphaeridium poculum, O. prolixispinosum, Palaeoperidinium cretaceum, Spinidinium styloniferum,* and *Surculosphaeridium longifurcatum,* which is characteristic for the Early Cretaceous. The assemblages correlate with the upper middle Albian *Chichaouadinium vestitum* Subzone to the lower upper Albian *Wigginsiella grandstandica* Subzone described from East Greenland by Nøhr-Hansen (1993) and recorded from the Canadian Arctic by Nøhr-Hansen and McIntyre (1998). The well sorted, fine-grained sediment, coal flasers, abundant bioturbation, and presence of dinoflagellate cysts suggest that Unit S-2 was deposited in a relatively calm shallow-marine environment. The angular form of grains and the high content of coal fragments indicate little physical reworking of the sediment before deposition, suggesting that deposition occurred proximally to the source of detritus. After deposition, the sediments in Hole SEG80B suffered little mechanical compaction and heating from the overburden.

IGNEOUS PETROLOGY

The volcanic basement was recovered from 41 holes at 33 sites along Transect EG65. The deepest recoveries were from Holes SEG22A (98 cm), SEG26A (110 cm), SEG27A (131 cm), SEG40A (118 cm), SEG60B (103 cm), and SEG61B (156 cm). The following observations and conclusions are drawn principally from igneous units, with additional information from basaltic clast units judged to sample local volcanic basement. Two distinctly different basalt series occur at Transect EG65, as detailed below.

The cored igneous units are dominantly massive, fine-grained, moderately to highly phyric basalts. Igneous units from Transect EG65 have diverse phenocryst assemblages composed of plagioclase as the volumetrically most abundant phenocryst and with or without minor amounts of clinopyroxene and olivine. Porphyritic to glomeroporphyritic (Fig. F11A) and seriate textures are common. Glomerophyric intergrowths occur with all three phenocrysts phases but are most common in the highly plagioclase phyric lavas. Indications for simultaneous growth are commonly seen in the form of "bow-tie" intergrowth between plagioclase and clinopyroxene (Fig. F11A). Plagioclase often retains a euhedral, lath-shaped fabric, whereas altered olivine often appears with subrounded to euhedral shapes (Fig. F11B). The groundmass is typically intergranular and intersertal and composed of plagioclase, clinopyroxene, opaque minerals (mostly Fe-Ti oxides and minor amounts of sulfides), and mesostasis. Slowly cooled, fine- to medium-grained groundmass interiors of flows and clasts show subophitic intergrowth between plagioclase laths and interstitial to granular clinopyroxene. Such flow interiors often retain a relatively fresh appearance (Fig. F11C). A weak trachytic groundmass texture defined by plagioclase laths is seen in many upper series basalts. Sparsely plagioclase phyric basalts are also common. These lavas often have large vesicles commonly filled with gray clay and zeolite (Fig. F11D).

F11. Lava textures, upper series, p. 39.

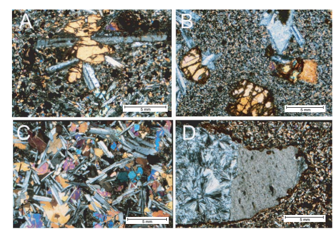

A less common suite of lavas contains olivine and plagioclase phenocrysts with minor amounts of clinopyroxene. These lavas are highly to moderately phyric and have a distinctive red coloration resulting from the alteration of olivine to iddingsite and lizardite (Fig. F12A). Chromium spinel occurs as inclusions in olivine phenocrysts (Fig. F12B) and in the groundmass of the most olivine-rich samples. Modal proportions of plagioclase and olivine phenocrysts are highly variable (Figs. F12C, F12D, F13). Small (<1 cm) xenoliths composed of olivine and green pyroxene (chromium diopside?) are reported in Unit I-1 from Holes SEG51B, SEG55B, and SEG55C.

F12. Lava textures, lower series, p. 40.

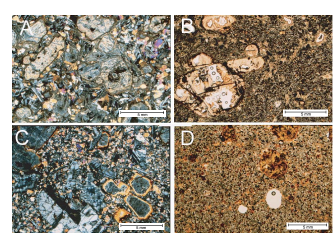

The occurrences of these two petrographically distinct suites of lavas (highly to moderately plagioclase phyric and highly to moderately olivine phyric), as illustrated by rock modes in Figure F13, form the basis for dividing the drilled lava succession into a lower series and an upper series. Sites landward of Site SEG51 are dominated by highly to moderately olivine-plagioclase phyric basalt, whereas basalt recovered seaward

F13. Phenocryst modes, p. 41.

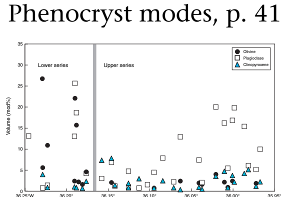

of Site SEG45 are typically aphyric to plagioclase-clinopyroxene phyric basalt.

Although most of the igneous units are described as massive, some show diffuse vesicle or amygdule bands (2–3 cm thick) roughly perpendicular to the core axis. Occasionally vesicles are flattened parallel to the banding (Holes SEG27A, SEG29A, SEG40A, and SEG44A). Rounded to highly irregularly shaped vesicles (0.5–4 mm in diameter) are present in most of the units. The vesicles may be elongated in bands or pipes (Fig. **F6**) and are either void or filled with secondary minerals (Fig. **F11**). Quartz, calcite, zeolite, and clay typically fill vesicles, vugs, and fractures. Rusty-brown weathered surfaces and fractures found on fragments in Units I-1 from Holes SEG52A and SEG63A may represent oxidized flow tops. Likewise, the highly fractured and crumbled basalt found at the top of Holes SEG45A and SEG51A resembles flow top rubble, whereas conjugate fracture sets and weakly developed slickensides described from Hole SEG21A suggest some postemplacement tectonic movement.

The contact between the sediment cover and the underlying basaltic basement is not preserved in any of the holes drilled from Transect EG65. The surface of the volcanic basement was preserved in two holes. Glacial striations are found on the top surface of core from Hole SEG40A. Remarkably, live corals attached to the glacially polished top surface were recovered from Hole SEG27A (see Fig. **F5**). Coral and other organisms attached to or coating larger pebbles and drilled basalt fragments and boulders from Hole SEG21A shows that certain portions of the seabed were void of fine-grained sediment covers.

It is also noteworthy that melanocratic gneiss was recovered in Hole SEG32A. Thin section examination shows an assemblage of hornblende, biotite, quartz, magnetite, ilmenite, and accessory zircon, apatite, sphene, and chalcopyrite (Fig. **F14**). Although no radiometric age information is available, the mineralogy and gneissic fabric of this cored basement are similar to the immediately adjacent onshore Precambrian crust.

F14. Melanocratic gneiss, p. 42.

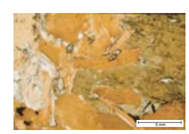

COMPOSITION OF IGNEOUS UNITS

Thirty-four igneous samples were analyzed by shore-based XRF procedures (Table **T2**). In addition to all I-1 units, we included a number of basaltic clasts of the C type (e.g., Holes SEG54A, SEG56A, SEG63A, and SEG76A) and one clast from Unit S-1 of Hole SEG64B, strongly suspected to sample the basement lithology at the site. Most of these samples have volatile contents between 0.5 and 1.5 wt% and low Fe_2O_3/FeO_{total} ratios. Notable exceptions are the sparsely to highly olivine phyric samples having volatile contents of 2–4 wt% and Fe_2O_3/FeO_{total} ratios > 0.5. All units are olivine normative and range between mildly nepheline normative to strongly hypersthene normative. Mildly nepheline normative basalt occurs exclusively in the upper series (Table **T2**).

T2. XRF data, p. 47.

The majority of igneous units are evolved tholeiitic basalt with Mg# < 0.52 and TiO_2 > 1.8 wt% (Fig. **F15**). Most are in the upper series, where the highly plagioclase phyric units tend to have the highest Mg number and lowest TiO_2 content. Basalts with Mg# > 0.65 and TiO_2 <1.0 wt% occur exclusively in lower series and correspond to the most olivine phyric units. The available trace element data show marked differences between upper and lower series lavas. For example, Ni (and also Cr and

F15. Element variations, p. 43.

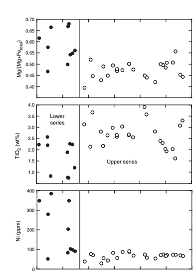

V) is most abundant in the highest Mg number lavas of the lower series (Fig. F15), whereas the incompatible element Zr is most abundant in the evolved basalts of the upper series. Sr is also elevated in the upper series lavas, but this may be because of the high modal proportion of plagioclase in many of these lavas.

PHENOCRYST COMPOSITIONS

The phenocryst compositions were determined by electron microprobe for the 34 igneous units. Table T3 provides average compositions for plagioclase, clinopyroxene, olivine, and chromian spinel. The full data set is presented in **"Appendix B,"** p. 13, of the "Explanatory Notes" chapter.

T3. Phenocryst composition, p. 49.

Plagioclase phenocrysts in the upper series lavas show large compositional ranges with average anorthite contents between An_{58} and An_{86}. Clinopyroxene coexisting with plagioclase has average Mg numbers between 0.70 and 0.81, although there is a poor correlation between the coexisting plagioclase and clinopyroxene compositions. Fresh olivine phenocrysts were found in only five samples and range in composition from Fo_{61} to Fo_{69}. The groundmass olivine in Unit I-1 of Hole SEG61B is the most iron-rich olivine analyzed (Fo_{54}).

Phenocrysts of the lower series olivine phyric lavas typically reach more primitive compositions than the upper series lavas. Plagioclase varies between An_{76} and An_{89} and clinopyroxene between Mg number 0.77 and 0.85. Fresh olivine was found in only two samples with composition ranging from Fo_{68} to Fo_{75}. Spinel has Cr/(Cr + Al + Fe^{3+}) ratios between 0.42 and 0.59, with the most Cr-rich spinels occurring as inclusions in olivine.

PALEOMAGNETIC RESULTS

A total of 48 intervals were studied from 36 sites along Transect EG65 to determine the magnetic polarity and whether some of the cored basaltic clasts were direct samples of basement or just loose and rotated clasts.

A typical demagnetization result is shown on a Zijderveld diagram in Figure F16. After removal of small secondary components related to viscous and/or drill-induced magnetization, the direction of the characteristic magnetic remanence is defined using standard principal component analysis (Kirschvink, 1980). Note that the azimuth of the drill cores is unknown; therefore, only the characteristic inclination is meaningful. Table T4 lists the demagnetization results, including characteristic inclination, intensity of natural remnant magnetization, magnetic susceptibility, and Königsberger ratio. Also given is the interpreted polarity together with important notes that are offered as a first interpretation of the paleomagnetic results.

F16. AF demagnetization, p. 44.

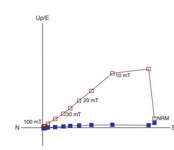

T4. Paleomagnetic results, p. 50.

Two intervals did not yield a reliable estimate of the characteristic inclination because of scattered demagnetization results (Holes SEG41A and SEG79C). Five intervals yielded intermediate inclinations. One of these intervals is from a loose basalt clast in Unit S-1 from Hole SEG39A. Four other intervals from Holes SEG44A, SEG45A, SEG74E, and SEG76A cannot easily be interpreted but possibly may represent short excursion events (Table T4). For all other intervals, the polarity is always of a reversed nature with a mean characteristic inclination of

–67.4° (N = 29, k = 24, α95 = 5.8°) using the method of McFadden and Reid (1982).

A total of seven units defined as cored clasts from Holes SEG23A, SEG42A, SEG55C, SEG74E, SEG75A, SEG76A, and SEG79C were examined. Of these only Unit C-1 from Hole SEG79C did not yield a polarity, whereas Units C-1 from Holes SEG74E and SEG76A indicate possible excursions similar to their neighboring holes and unequivocally sampled basement. Unit C-1 from Hole SEG55C gives a normal inclination, opposite in direction to all neighboring holes, and we surmise that this clast had been transposed in the core box. The remaining C-units gave inclinations consistent with the neighboring holes and suggest that these represent in situ basaltic basement as sampled in Holes SEG23A, SEG42A, and SEG75A.

CORE AND THIN SECTION DESCRIPTIONS

Brief lithologic descriptions of all recovered cores and thin section descriptions from sites drilled along Transect EG68, as well as digital core photographs taken onboard, are included on summary sheets in **Supplementary Material.** The same information can be obtained from the ODIN database (see **"ODIN Database,"** p. 9, in the "Explanatory Notes" chapter) available from the authors.

REFERENCES

Holbrook, W.S., Larsen, H.C., Korenaga, J., Dahl-Jensen, T., Reid, I.D., Kelemen, P.B., Hopper, J.R., Kent, G.M., Lizarralde, D., Bernstein, S., and Detrick, R., 2001. Mantle thermal structure and active upwelling during continental breakup in the North Atlantic. *Earth Planet. Sci. Lett.,* 190(3–4):251–266. **doi:10.1016/S0012-821X(01)00392-2**

Kirschvink, J.L., 1980. The least-squares line and plane and the analysis of palaeomagnetic data. *Geophys. J. R. Astron. Soc.,* 62(3):699–718.

Larsen, H.C., Saunders, A.D., Clift, P.D., et al., 1994. *Proc. ODP, Init. Repts.,* 152: College Station, TX (Ocean Drilling Program). **doi:10.2973/odp.proc.ir.152.1994**

McFadden, P.L., and Reid, A.B., 1982. Analysis of paleomagnetic inclination data. *Geophys. J. R. Astron. Soc.,* 69:307–319.

Nøhr-Hansen, H., 1993. Dinoflagellate cyst stratigraphy of the Barremian to Albian, Lower Cretaceous, North-East Greenland. *Bull. Groenl. Geol. Unders.,* 166.

Nøhr-Hansen, H., and McIntyre, D.J., 1998. Upper Barremian to upper Albian (Lower Cretaceous) dinoflagellate cyst assemblages, Canadian Arctic archipelago. *Palynology*, 22:143–166.

Figure F1. Transect EG65 area. Thin lines = H/S *Dana* reflection seismic lines (Hopper et al., 1997), thick lines = SIGMA II line (Holbrook et al., 2001). Sparker Line DLC99-3 (shown in detail in Figs. F3, p. 28, and F4, p. 29) is located along Line DLC9709 (shown in Fig. F2, p. 27). Intersections of short lines crossing the sparker line mark the location of drill sites in the inner and outer drilling areas. TEST02 = sparker test line acquired in Sermiligaq Fjord during inclement weather.

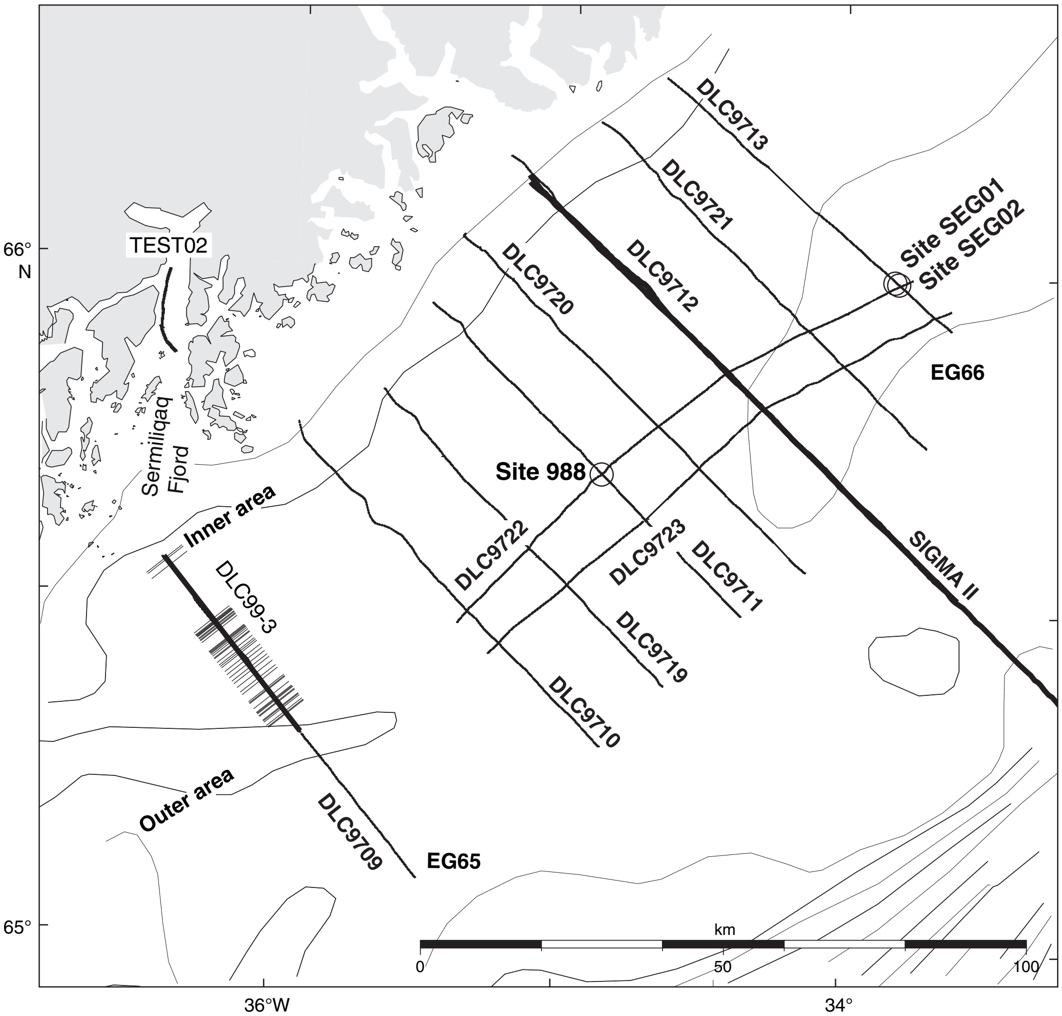

Figure F2. Reflection seismic Line DLC9709 (Hopper et al., 1997). Inner and outer areas and extent of the corresponding sparker seismic Line DLC99-3 are marked on top with a key to corresponding figures. Positions of drill sites shown as thin vertical lines. Three multiples can be seen lower in the section.

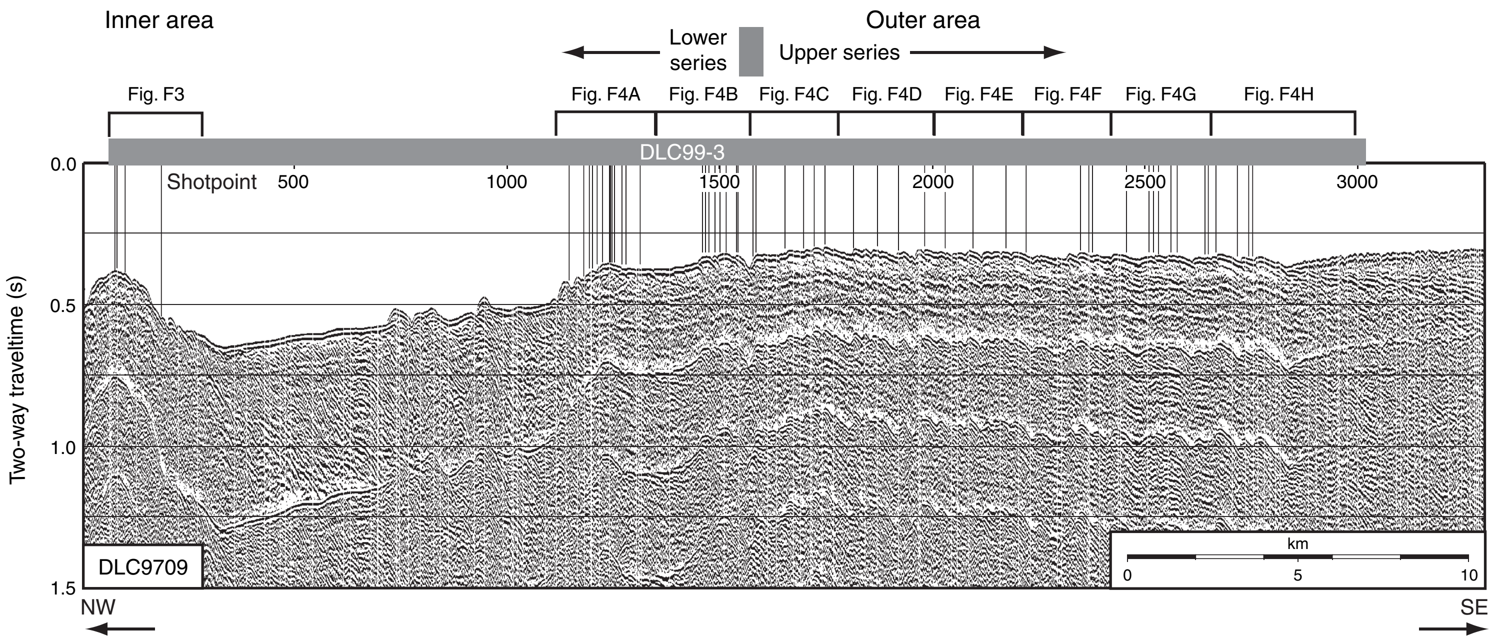

Figure F3. Single-channel sparker Line DLC99-3 of inner area. Line collected between 65°33.451′N, 36°25.320′W and 65°18.563′N, 35°55.276′W. Length of line is 36 km, including the segment between the inner and outer profiles not shown on figure. TRC = trace sequence number from 0 (beginning of line) to 14,000 (Table T1, p. 45). 1 km = 400 TRC.

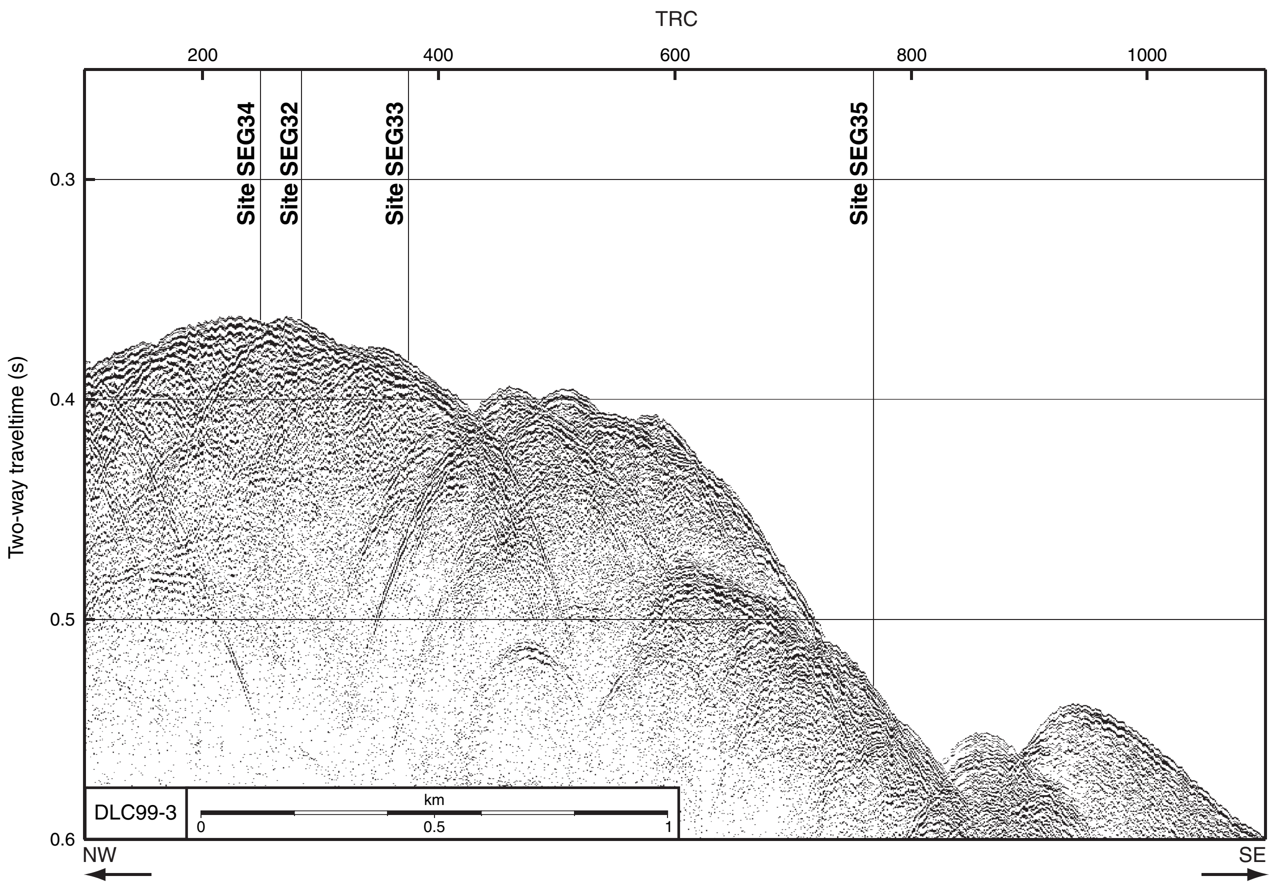

Figure F4. Single-channel sparker Line DLC99-3 of outer area. TRC = trace sequence number along line (Table T1, p. 45). See caption for Figure F3, p. 28. **A.** 5000–6000 TRC. **B.** 6000–7000 TRC. (Continued on next three pages.)

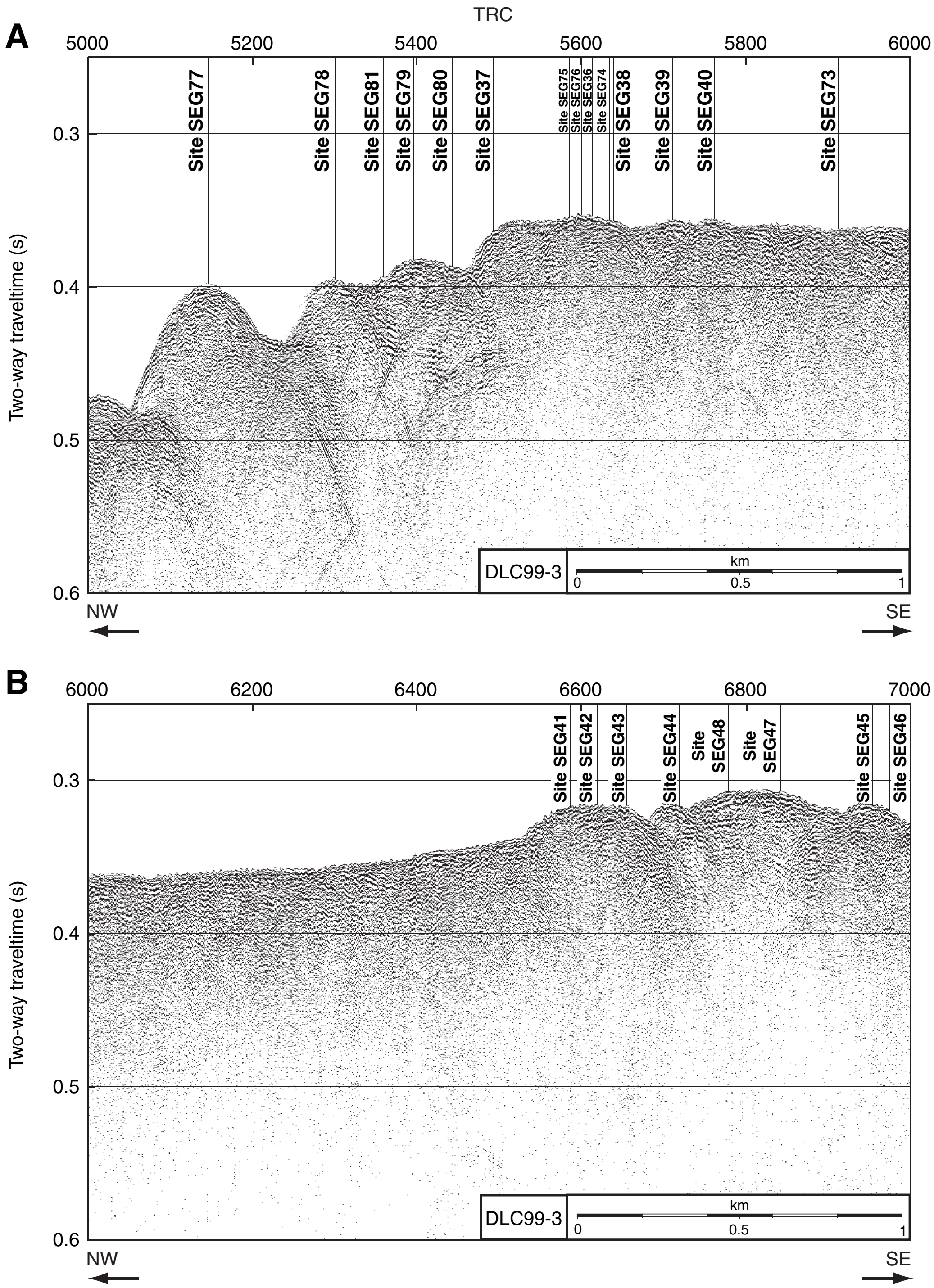

Figure F4 (continued). C. 7000–8000 TRC. D. 8000–9000 TRC. (Continued on next page.)

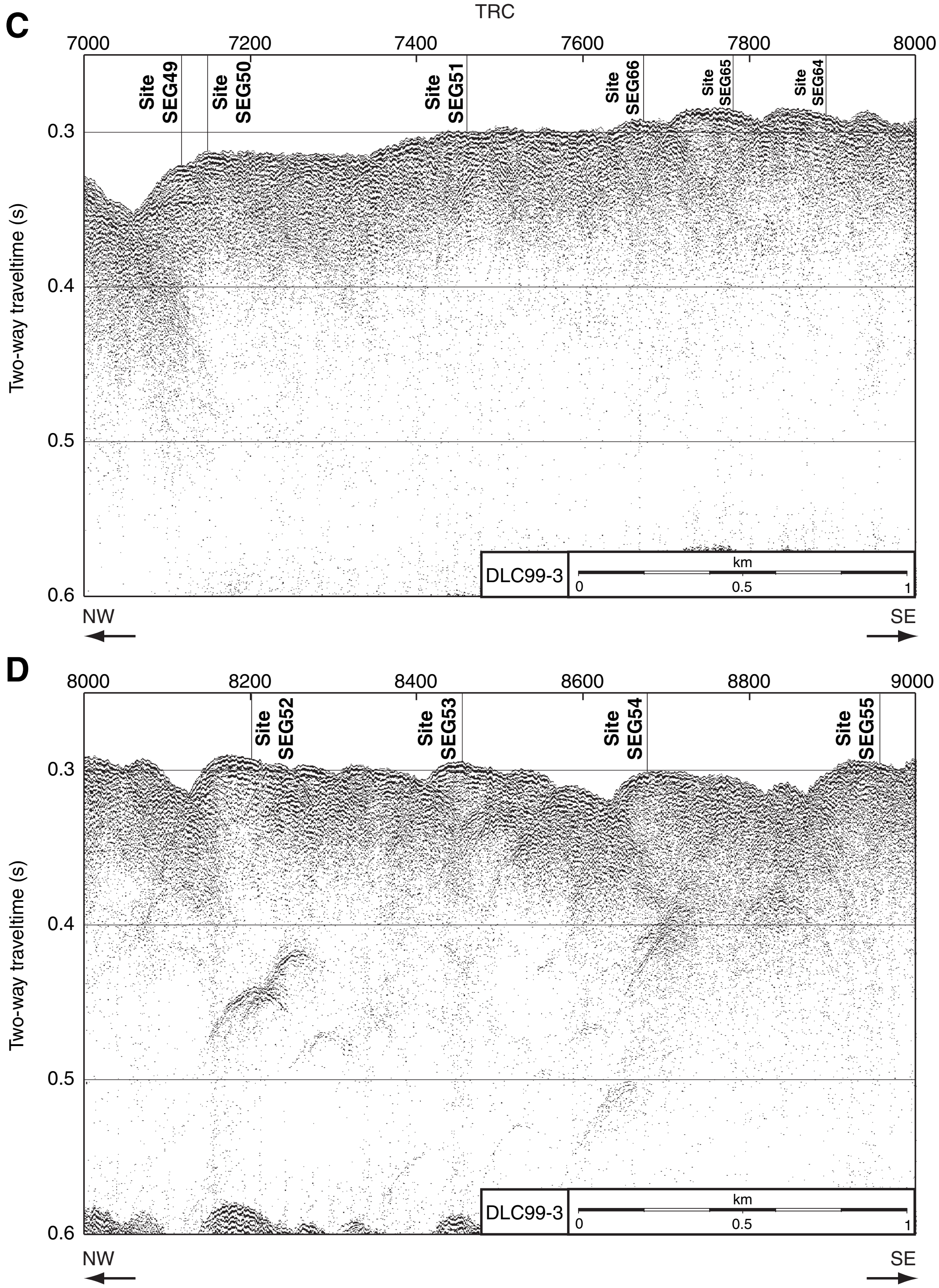

Figure F4 (continued). E. 9,000–10,000 TRC. F. 10,000–11,000 TRC. (Continued on next page.)

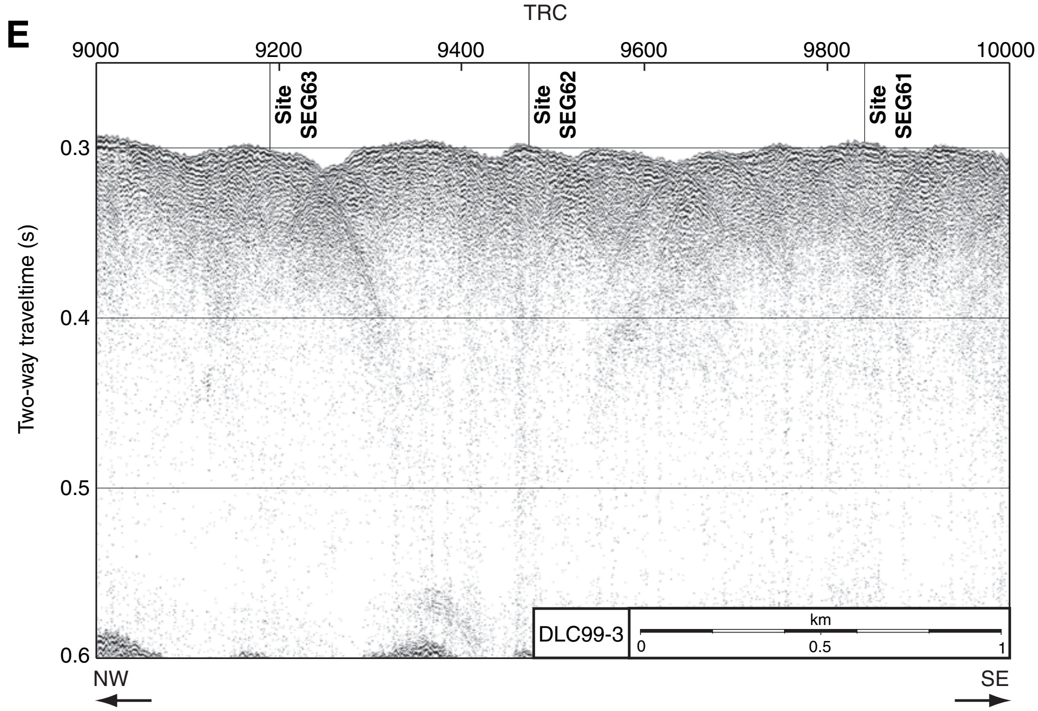

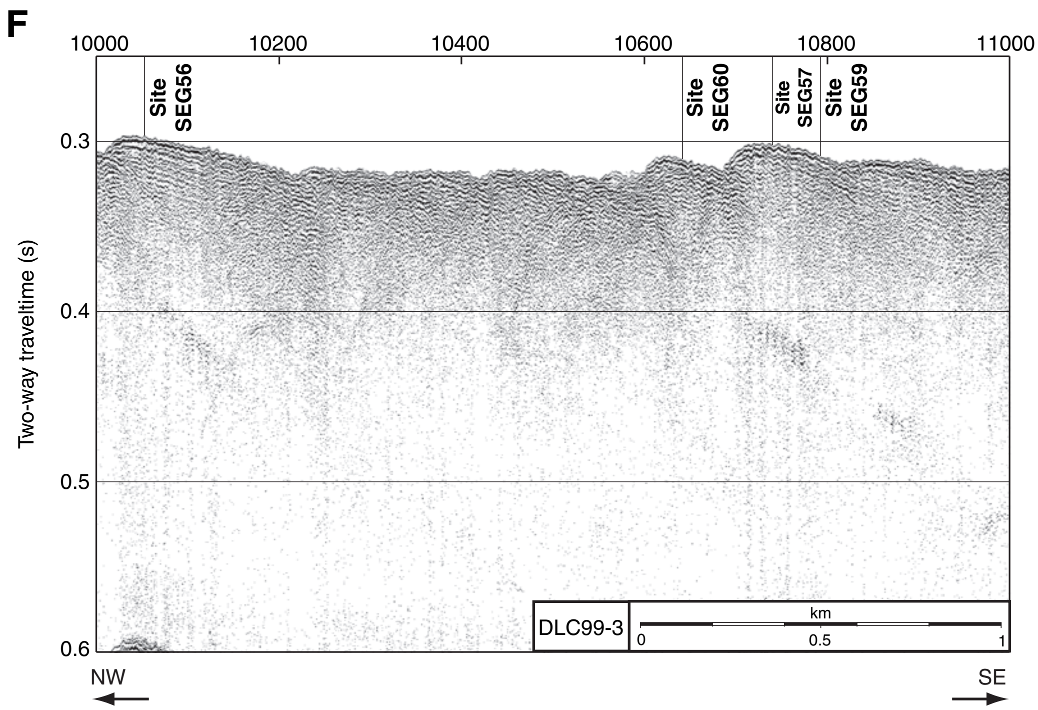

Figure F4 (continued). G. 11,000–12,000 TRC. **H.** 12,000–13,000 TRC.

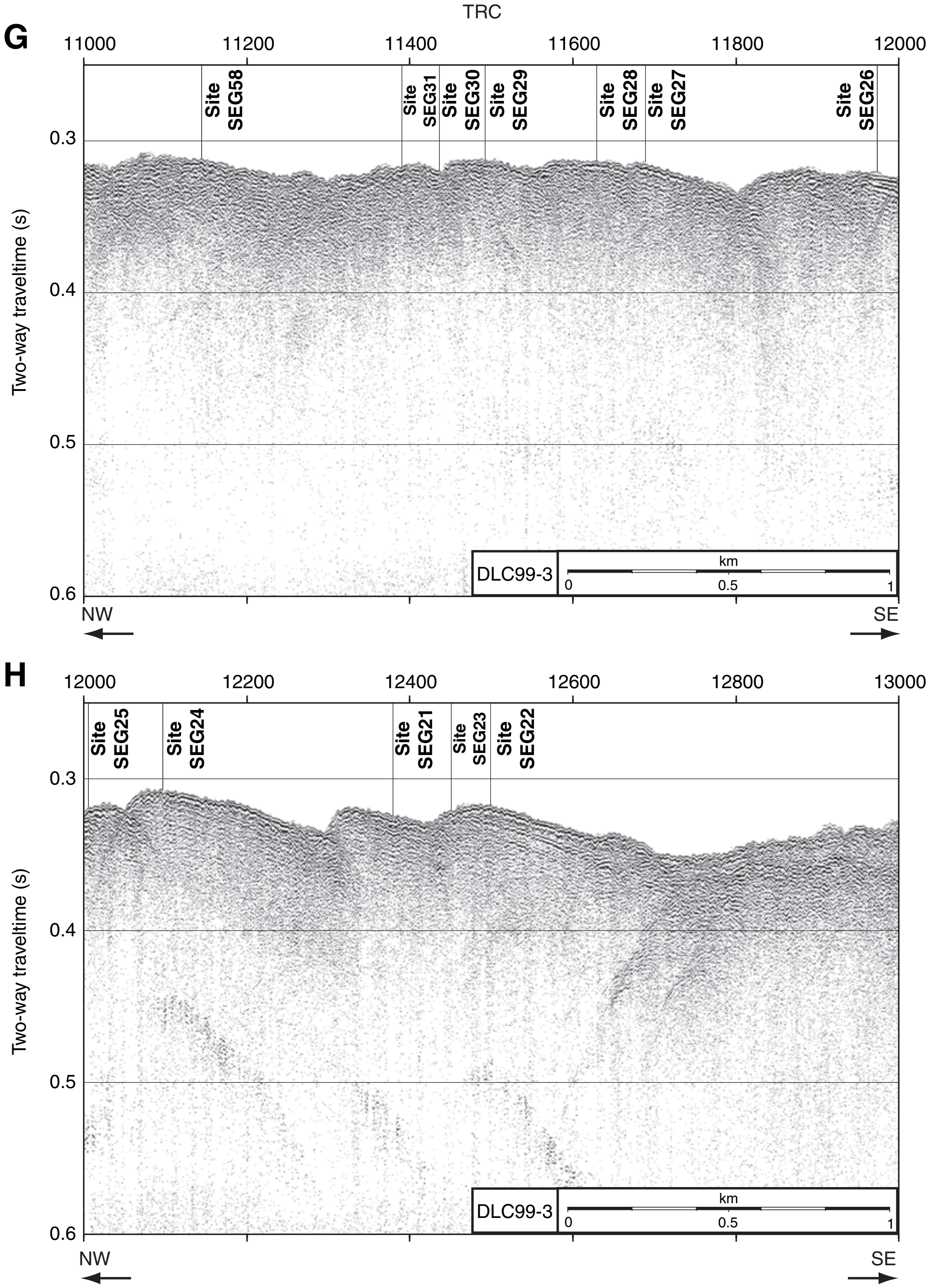

Figure F5. Cold-water corals growing on bare, glacially polished, volcanic basement recovered undamaged from Hole SEG27A.

Figure F6. Pipe vesicle in interval 163X-SEG31A-1-1, 0–20 cm. Arrow indicates up direction. Core is 20 cm long.

Figure F7. Largely intact core of friable sandstone of Unit S-2, Hole SEG80B.

Figure F8. Sand-size fraction of diamicton matrix from Unit S-1, Hole SEG48A. **A.** Dominantly angular quartz and basalt fragments and a single foraminifer shell (plane-polarized light). **B.** Same view in cross-polarized light revealing the alkali feldspar grain in the center of view.

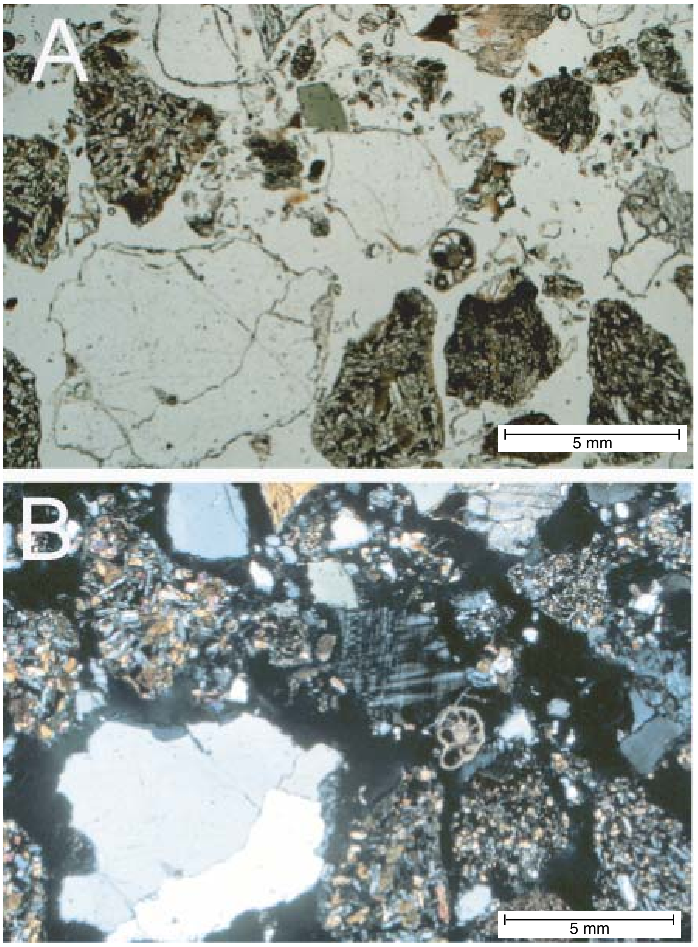

Figure F9. Thin section of consolidated quartzwacke from Unit S-1 (Sample 163X-SEG38B-1-1, 8–12 cm) (plane-polarized light). Note fine-grained, moderately well sorted, low-sphericity quartz and flakes of carbon cemented by calcite.

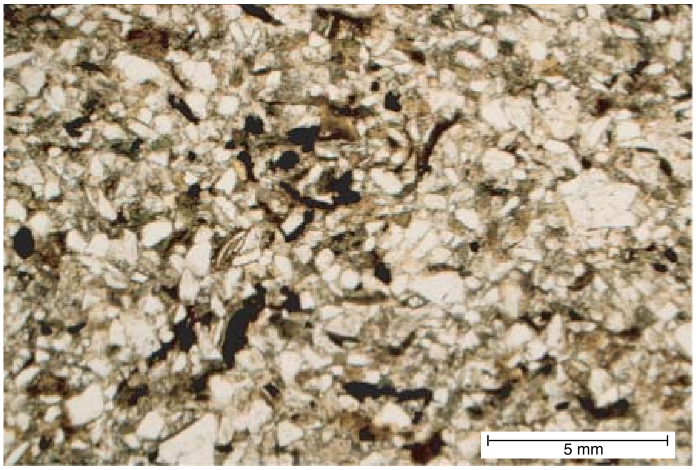

Figure F10. Fine-grained arkosic sandstone from Unit S-2, Hole SEG80B. **A.** Clear, dominantly angular quartz and feldspar grains with minor organic grains (opaque) and elongate mica grains (red brownish) (plane-polarized light). Clear alkali feldspar overgrowths on dusty cores are common. The limited deformation of mica grains suggests low amounts of mechanical compaction. The high porosity value of ~30% reflects the low compaction and widespread feldspar dissolution. **B.** Same view in cross-polarized light. Untwinned alkali feldspar overgrowths are cemented by sporadic calcite with high birefringence.

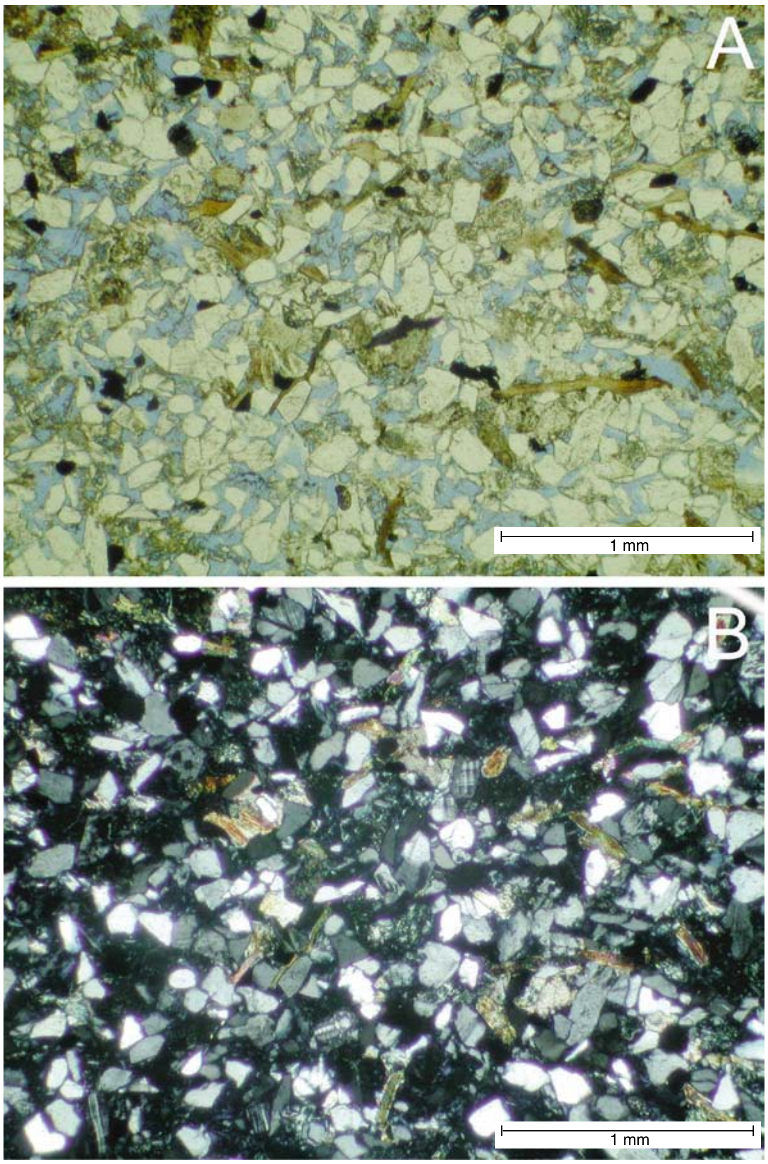

Figure F11. Typical mineralogy and textures of upper series lavas. **A.** Bow-tie intergrowth of plagioclase and clinopyroxene of a moderately plagioclase-olivine-clinopyroxene phyric basalt (Unit I-1; Sample 163X-SEG57A-1-1, 18–22 cm). The groundmass is composed of the same mineral phases and Fe-Ti oxides. **B.** Seriate, highly plagioclase-olivine-clinopyroxene phyric basalt with euhedral plagioclase and subhedral (partially altered) olivine (Unit I-1; Sample 163X-SEG58A-1-1, 9–13 cm). **C.** Fresh, granular to subophitic groundmass of basaltic clast (Unit C-1; Sample 163X-SEG64B-1-1, 0–4 cm). Plagioclase laths, granular to interstitial clinopyroxene, and Fe-Ti oxide minerals dominate. **D.** Vesicular and sparsely plagioclase phyric basalt. Large vesicle filled with gray clay and zeolite (Unit I-1; Sample 163X-SEG55B-1-1, 27–31 cm).

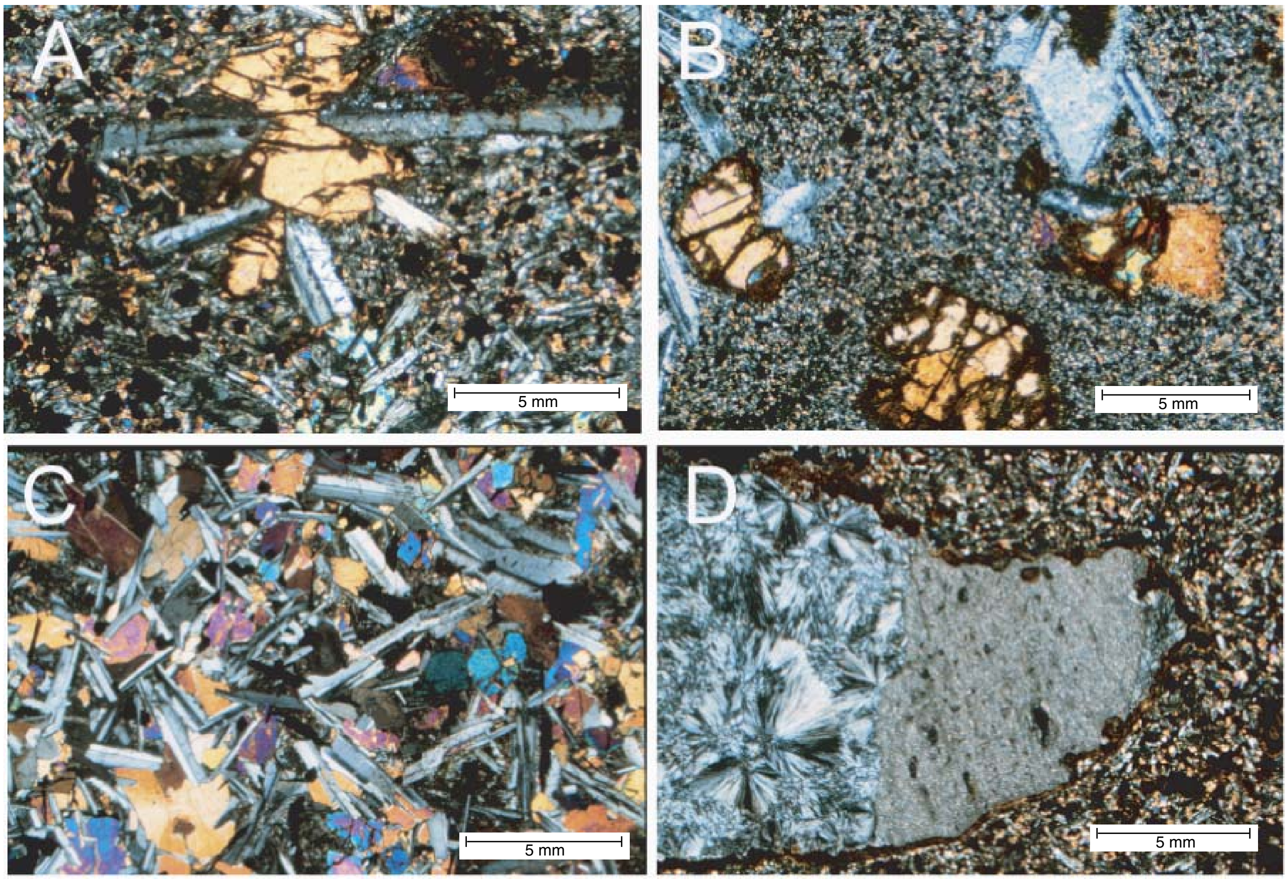

Figure F12. Typical mineralogy and textures of lower series lavas. **A.** Highly olivine phyric basalt (Sample 163X-SEG76B-1-1, 0–4 cm). Equant to elongate olivine phenocrysts with chromian-spinel inclusions are completely replaced. **B.** Laths of plagioclase and prismatic olivine with inclusions of chromian-spinel replaced by iddingsite in a very fine grained groundmass of plagioclase, Fe-Ti oxides, and altered mesostasis (Sample 163X-SEG77A-1-1, 22–26 cm). **C.** Olivine-plagioclase-clinopyroxene phyric basalt (Sample 163X-SEG43A-1-1, 11–15 cm). Olivine altered to iddingsite, whereas clinopyroxene is fresh. **D.** Vesicular and aphyric basalt (Sample 163X-SEG76A-1-1, 8–10 cm). Note vesicles are either open or filled by gray clay.

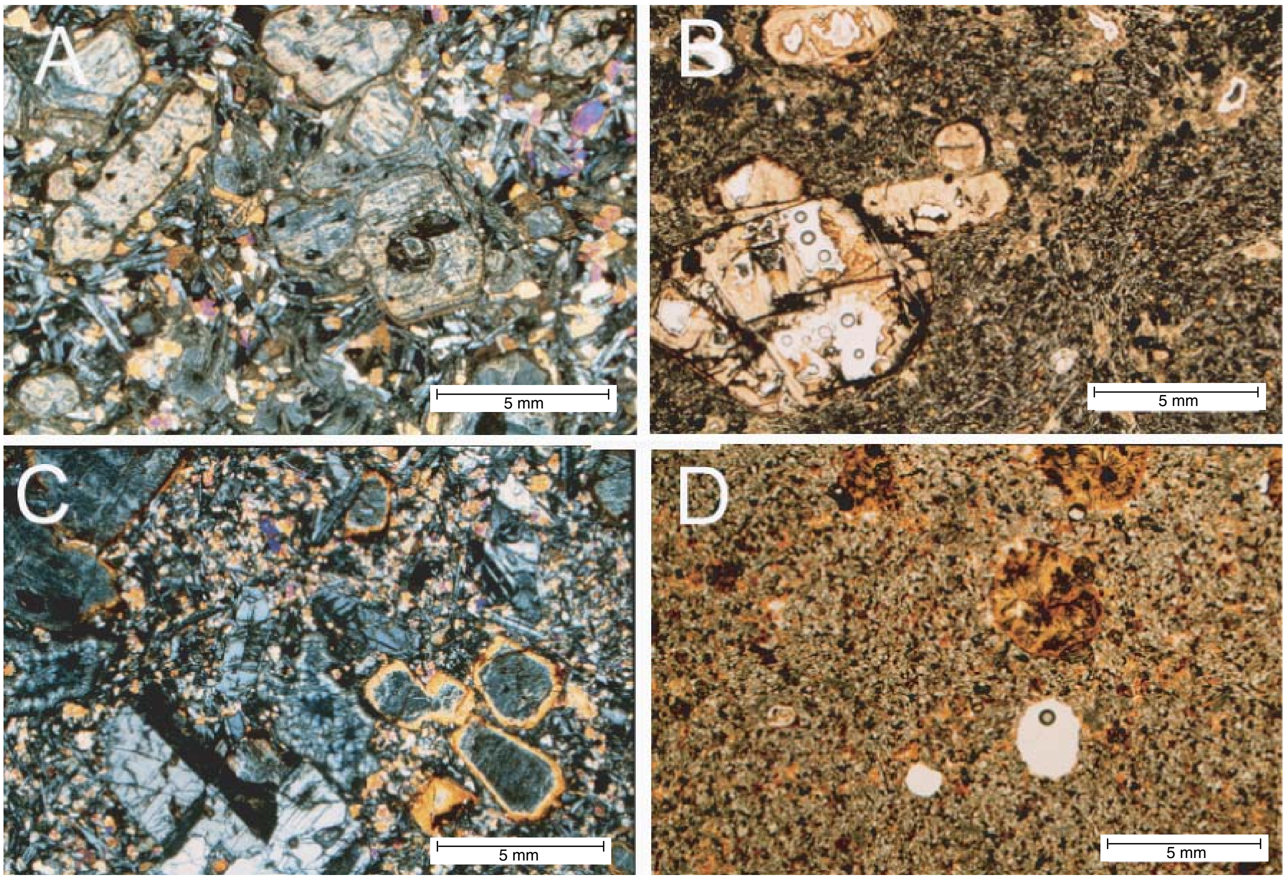

Figure F13. Modes of plagioclase, clinopyroxene, and olivine phenocrysts in lavas from Transect EG65. The high modal abundances of olivine and plagioclase are used to define a lower and an upper series, respectively. The boundary is placed between Sites SEG45 and SEG51 at ~36°17′W.

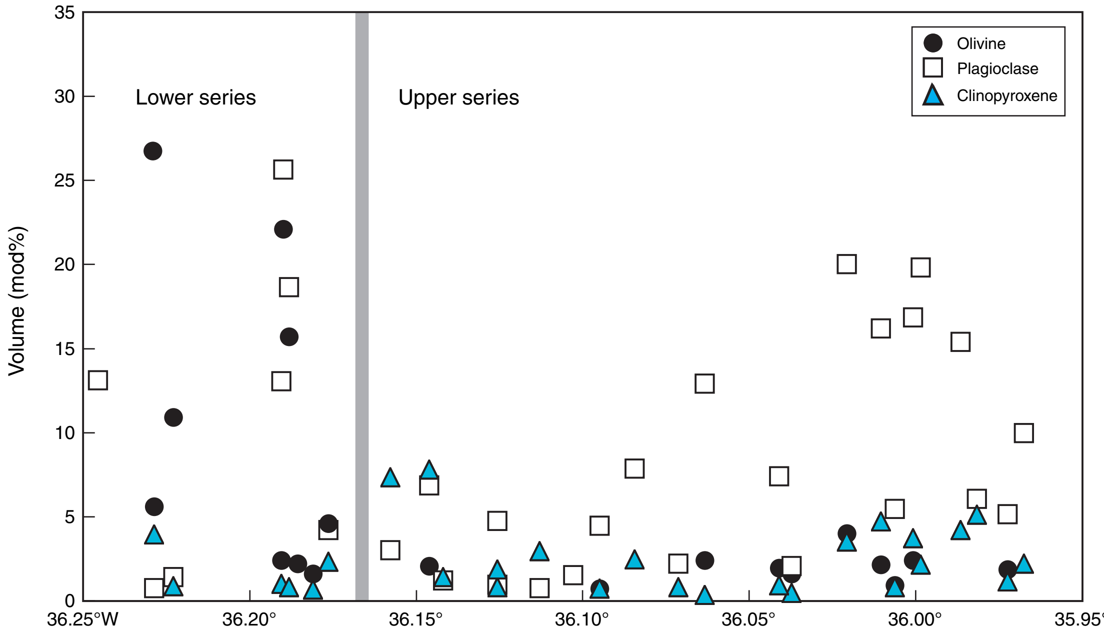

Figure F14. Melanocratic gneiss recovered from Hole SEG32A (Sample 163X-SEG32A-1-1, 21–23 cm). Orange shades = mica and amphibole. Needles of apatite and stubby zircon are evident. Trace amounts of Fe-Ti oxide minerals also present.

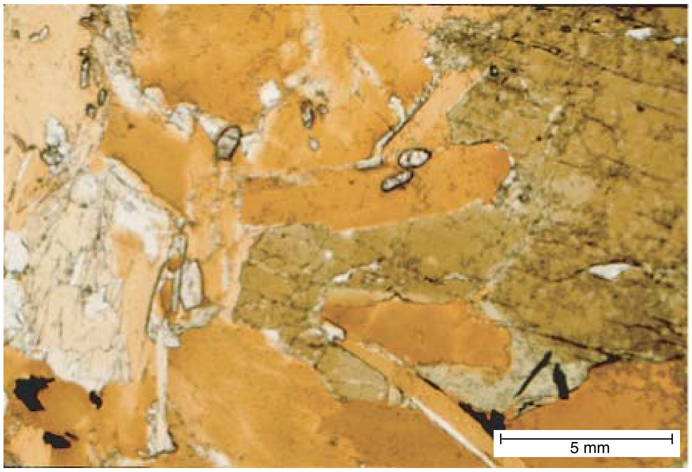

Figure F15. Mg/(Mg + Fe_{total}), TiO_2, and Ni variations in lavas from Transect EG65. The geographic distribution of the upper and lower series is taken from Figure **F13**, p. 41.

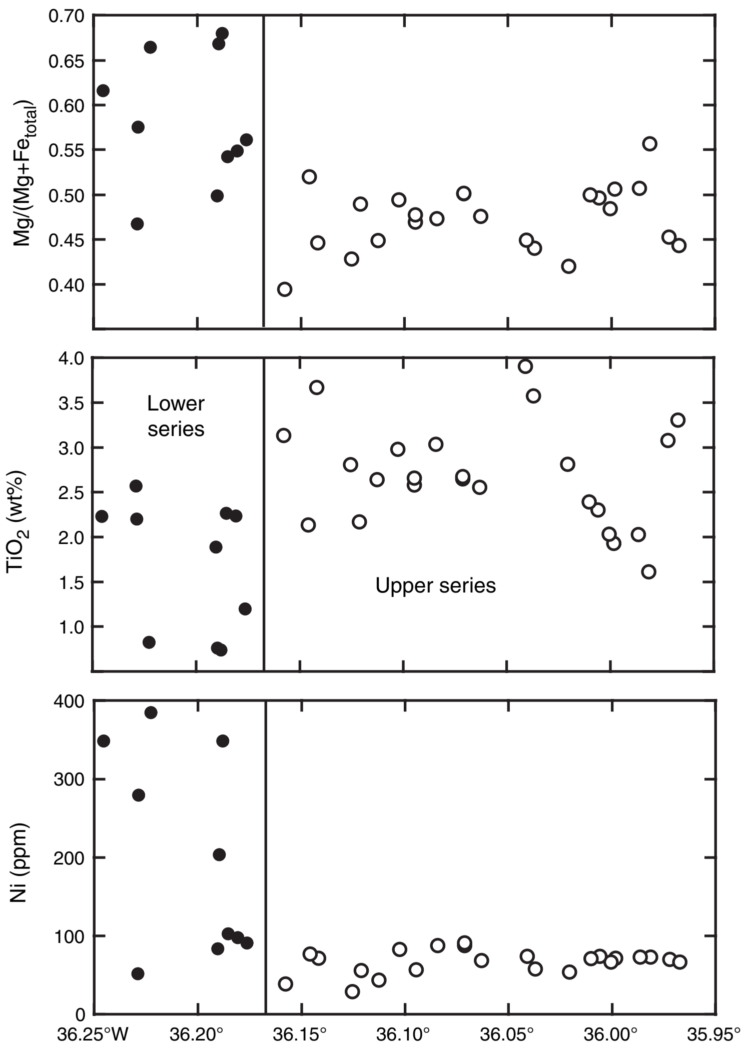

Figure F16. Response of Sample 163X-SEG27A1-1, 45–48 cm, to alternating-field demagnetization. Solid symbols = points on the horizontal plane, open symbols = points on the vertical plane, NRM = natural remanent magnetization.

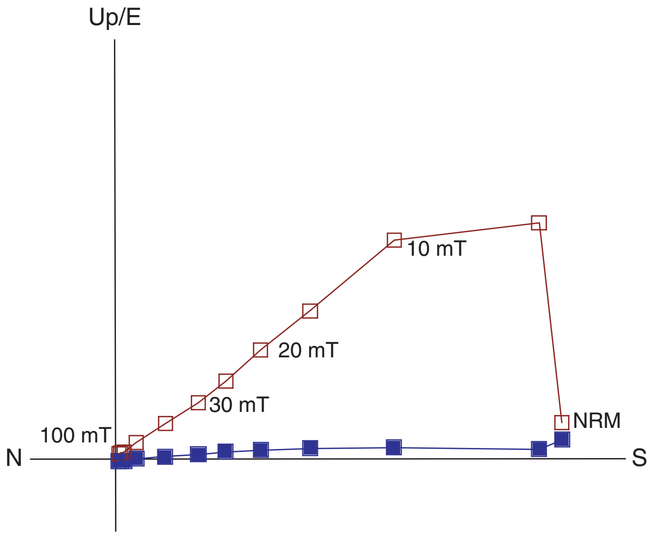

Table T1. Transect EG65 core summaries. (See table notes. Continued on next page.)

Core	UTC Date (Aug 1999)	UTC Time (hr)	Position Latitude	Position Longitude	Sparker line TRC	Air gun line shotpoint	Water depth (m)	Rock coring intervals (mbsf) Top	Rock coring intervals (mbsf) Bottom	Core recovery (m)
163X-										
SEG21A-1	2	1544	65°20.057′N	35°58.338′W	12336	2719	231.30	0.35	0.51	0.18
SEG21B-1	2	1622	65°20.054′N	35°58.339′W	12336	2719	229.64	0.38	0.44	0.17
SEG21C-1	2	1710	65°20.058′N	35°58.340′W	12336	2719	230.08	0.39	0.54	0.12
SEG21D-1	2	1846	65°20.056′N	35°58.339′W	12336	2719	231.25	0.28	0.58	0.38
SEG22A-1	2	2038	65°19.862′N	35°57.944′W	12500	2758	229.96	0.29	1.15	0.98
SEG23A-1	2	2319	65°19.914′N	35°58.045′W	12454	2747	233.92	0.50	0.72	0.23
SEG24A-1	3	0112	65°20.323′N	35°58.897′W	12105	2664	224.15	0.40	0.90	0.57
SEG25A-1	3	0456	65°20.420′N	35°59.126′W	12017	2644	213.73	0.50	1.09	0.15
SEG26A-1	3	0619	65°20.454′N	35°59.191′W	11986	2637	233.29	0.30	1.39	1.10
SEG27A-1	3	1000	65°20.803′N	35°59.904′W	11689	2568	228.98	0.18	1.22	1.31
SEG28A-1	3	1232	65°20.885′N	36°0.052′W	11627	2551	229.48	0.29	0.85	0.48
SEG29A-1	3	1441	65°21.042′N	36°0.377′W	11494	2520	227.96	1.40	2.12	0.65
SEG30A-1	3	1655	65°21.107′N	36°0.510′W	11440	2508	230.96	0.57	1.52	0.23
SEG31A-1	3	1846	65°21.156′N	36°0.626′W	11396	2498	228.79	0.66	1.36	0.70
SEG32A-1	3	1217	65°33.051′N	36°25.479′W	284	78	270.53	0.80	1.32	0.23
SEG32B-1	3	1420	65°33.054′N	36°25.485′W	284	78	272.08	0.82	1.82	0.22
SEG33A-1	3	1613	65°32.987′N	36°25.270′W	365	93	276.31	0.60	2.06	0.00
SEG34A-1	3	1822	65°33.081′N	36°25.557′W	250	73	266.28	0.63	0.68	0.00
SEG35A-1	3	2029	65°32.561′N	36°24.370′W	770	196	382.37	1.88	3.00	0.13
SEG36A-1	3	2030	65°27.455′N	36°13.722′W	5612	1218	257.26	0.60	0.86	0.25
SEG37A-1	5	0018	65°27.571′N	36°13.975′W	5495	1192	264.27	1.40	3.00	0.07
SEG38A-1	5	0137	65°27.420′N	36°13.642′W	5637	1225	262.40	0.00	0.00	0.00
SEG38B-1	5	0220	65°27.425′N	36°13.648′W	5637	1225	261.97	0.91	1.88	0.32
SEG38C-1	13	0923	65°27.423′N	36°13.646′W	5637	1225	263.14	1.28	1.85	0.07
SEG39A-1	5	0449	65°27.342′N	36°13.480′W	5709	1243	261.64	0.60	1.19	0.12
SEG40A-1	5	0607	65°27.284′N	36°13.374′W	5759	1256	257.85	0.65	1.89	1.18
SEG41A-1	5	1013	65°26.351′N	36°11.432′W	6588	1447	228.41	0.00	0.42	0.23
SEG42A-1	5	1135	65°26.321′N	36°11.374′W	6620	1453	229.71	0.58	1.14	0.13
SEG42B-1	5	1241	65°26.321′N	36°11.375′W	6620	1453	229.73	0.95	1.40	0.37
SEG42C-1	5	1429	65°26.324′N	36°11.399′W	6620	1453	229.72	1.39	1.91	0.48
SEG43A-1	5	1807	65°26.278′N	36°11.290′W	6656	1462	229.46	0.62	1.12	0.47
SEG44A-1	5	2049	65°26.207′N	36°11.136′W	6720	1476	228.48	0.26	0.72	0.46
SEG45A-1	5	2333	65°25.952′N	36°10.589′W	6946	1532	227.95	0.48	1.12	0.49
SEG46A-1	6	0150	65°25.944′N	36°10.558′W	6959	1534	228.64	0.82	0.92	0.22
SEG47A-1	6	0352	65°26.074′N	36°10.855′W	6837	1505	223.33	0.52	0.96	0.75
SEG48A-1	6	0619	65°26.152′N	36°11.021′W	6775	1488	225.22	1.90	2.11	0.71
SEG49A-1	6	0756	65°25.769′N	36°10.231′W	7114	1577	232.20	0.79	1.46	0.50
SEG50A-1	6	1005	65°25.736′N	36°10.170′W	7148	1585	226.87	1.66	1.77	0.33
SEG51A-1	6	1131	65°25.415′N	36°9.470′W	7455	1665	217.59	0.42	0.59	0.52
SEG51B-1	6	1244	65°25.417′N	36°9.471′W	7455	1665	217.59	0.41	0.56	0.23
SEG51C-1	6	1403	65°25.416′N	36°9.472′W	7455	1665	217.20	0.44	0.92	0.45
SEG52A-1	6	1708	65°24.620′N	36°7.841′W	8200	1846	212.45	0.28	0.46	0.31
SEG53A-1	6	2034	65°24.363′N	36°7.281′W	8451	1891	214.98	0.37	0.60	0.22
SEG53B-1	6	2238	65°24.363′N	36°7.280′W	8451	1891	213.67	0.36	0.72	0.33
SEG54A-1	7	0047	65°24.110′N	36°6.779′W	8683	1934	216.94	0.44	0.71	0.22
SEG55A-1	7	0238	65°23.828′N	36°6.171′W	8964	1983	214.75	0.50	0.00	0.00
SEG55B-1	7	0500	65°23.829′N	36°6.172′W	8964	1983	214.59	0.60	0.98	0.33
SEG55C-1	7	0725	65°23.828′N	36°6.168′W	8964	1983	214.17	0.15	0.32	0.13
SEG56A-1	7	1419	65°22.684′N	36°3.803′W	10057	2194	216.24	0.30	0.71	0.35
SEG56B-1	7	1646	65°22.689′N	36°3.808′W	10057	2194	217.22	0.37	0.60	0.19
SEG57A-1	7	1850	65°21.940′N	36°2.235′W	10742	2341	219.78	0.48	0.87	0.45
SEG58A-1	7	2249	65°21.463′N	36°1.246′W	11146	2436	218.74	0.57	1.13	0.27
SEG59A-1	8	0200	65°21.890′N	36°2.136′W	10774	2351	222.00	0.40	0.80	0.16
SEG59B-1	8	0314	65°21.889′N	36°2.138′W	10774	2351	224.48	0.32	0.32	0.16
SEG60A-1	8	0439	65°22.044′N	36°2.461′W	10645	2321	213.84	0.42	0.51	0.03
SEG60B1	8	0631	65°22.045′N	36°2.462′W	10645	2321	213.90	0.35	1.35	1.03
SEG61A1	8	1053	65°22.911′N	36°4.276′W	9836	2151	217.92	0.36	0.82	0.81
SEG61B1	8	1323	65°22.911′N	36°4.279′W	9836	2151	262.40	0.30	1.67	1.56
SEG62A1	8	1721	65°23.282′N	36°5.066′W	9478	2082	217.66	0.42	0.94	0.42
SEG63A1	8	2028	65°23.594′N	36°5.699′W	9183	2024	215.32	0.82	1.01	0.30
SEG63B1	8	2226	65°23.590′N	36°5.690′W	9183	2024	207.63	0.48	0.91	0.65
SEG64A1	9	0124	65°24.947′N	36°8.522′W	7894	1779	208.52	0.48	0.65	0.17
SEG64B1	9	0250	65°24.951′N	36°8.517′W	7894	1779	209.64	0.30	0.87	0.08
SEG65A1	9	0447	65°25.067′N	36°8.762′W	7786	1752	208.38	0.40	0.68	0.31
SEG65B1	9	0642	65°25.065′N	36°8.765′W	7786	1752	212.79	0.25	0.57	0.30
SEG66A1	9	0910	65°25.19′N	36°9.026′W	7661	1722	641.60	0.30	0.60	0.16

Table T1 (continued).

Core	UTC Date (Aug 1999)	UTC Time (hr)	Position Latitude	Position Longitude	Sparker ine TRC	Air gun line shotpoint	Water depth (m)	Rock coring intervals (mbsf) Top	Rock coring intervals (mbsf) Bottom	Core recovery (m)
SEG73A1	11	1658	65°27.112′N	36°12.992′W	5923	1293	263.40	0.85	1.13	0.00
SEG73B1	11	1752	65°27.110′N	36°12.993′W	5923	1294	263.30	0.00	3.00	0.14
SEG74A1	11	1930	65°27.424′N	36°13.655′W	5631	1224	261.00	1.60	1.93	0.00
SEG74B1	11	2131	65°27.433′N	36°13.656′W	5631	1224	574.80	1.10	1.20	0.21
SEG74C1	11	2302	67°27.431′N	36°13.672′W	5631	1224	260.00	0.43	0.51	0.00
SEG74D1	12	0004	65°27.431′N	36°13.67′W	5631	1224	259.50	0.71	1.01	0.17
SEG74E1	12	0140	65°27.431′N	36°13.668′W	5631	1224	256.94	0.87	2.40	0.07
SEG75A1	12	0313	65°27.482′N	36°13.776′W	5590	1212	257.96	1.68	1.94	0.26
SEG75B1	12	0432	65°27.482′N	36°13.779′W	5590	1212	260.45	1.68	1.93	0.30
SEG75C1	12	0650	65°27.481′N	36°13.772′W	5590	1212	259.08	1.40	1.92	0.45
SEG76A1	12	1121	65°27.469′N	36°13.750′W	5596	1215	257.45	0.30	0.41	0.11
SEG76B1	12	1232	65°27.469′N	36°13.753′W	5596	1215	291.77	1.12	1.40	0.21
SEG77A1	12	1606	65°27.938′N	36°14.738′W	5143	1112	294.98	0.66	1.07	0.51
SEG77B1	12	2002	65°27.939′N	36°14.740′W	5143	1112	287.00	0.40	0.60	0.35
SEG77C1	12	2201	65°27.937′N	36°14.728′W	5143	1112	287.00	0.56	1.47	0.49
SEG78A1	13	0111	65°27.774′N	36°14.412′W	5295	1148	279.52	0.00	0.00	0.00
SEG79A1	13	0552	65°27.681′N	36°14.218′W	5396	1168	280.88	0.56	0.82	0.00
SEG79B1	13	0659	65°27.680′N	36°14.219′W	5396	1168	280.77	0.32	0.32	0.00
SEG79C1	13	0800	65°27.675′N	36°14.208′W	5396	1168	263.14	0.58	0.68	0.25
SEG80A1	13	1140	65°27.672′N	36°14.102′W	5449	1170	287.02	1.88	1.88	0.05
SEG80B1	13	1251	65°27.671′N	36°14.101′W	5449	1170	286.60	2.54	3.00	0.64
SEG81A1	13	1514	65°27.714′N	36°14.284′W	5361	1161	288.92	0.00	1.88	0.11
SEG81B1	13	1653	67°27.710′N	36°14.278′W	5361	1161	287.89	1.36	1.89	0.00

Notes: Sparker Line DLC99-3, air gun Line DLC9709. UTC = Universal Time Coordinated. TRC = trace sequence number along the line (see Fig. F3, p. 28).

Table T2. Representative X-ray fluorescence element data, Transect EG65. (Continued on next page.)

Core, section, interval (cm)	Series	Unit	Major element oxides (wt%)												Iron oxide (wt%)			CIPW (wt%)	
			SiO_2	TiO_2	Al_2O_3	FeO*	MnO	MgO	CaO	Na_2O	K_2O	P_2O_5	LOI	Total	Fe_2O_3	FeO	Mg#	Hy	Ne
163X-																			
SEG21D-1-1 (Piece 1A, 9–18)	Upper	I-1	47.37	3.12	13.63	13.69	0.21	6.36	10.73	2.85	0.30	0.31	1.43	99.49	5.48	8.61	0.453	4.4	
SEG22A-1-1 (Piece 3A, 15–22)	Upper	I-1	47.17	3.34	13.74	13.80	0.21	6.17	10.71	2.89	0.32	0.33	1.33	99.73	5.97	8.30	0.444	3.6	
SEG24A-1-1 (Piece 2, 4–12)	Upper	I-1	48.60	1.63	14.79	11.15	0.19	7.87	11.70	2.28	0.23	0.14	1.41	99.56	4.29	7.19	0.557	10.7	
SEG26A-1-1 (Piece 6G, 85–92)	Upper	I-1	48.76	2.04	15.38	11.74	0.19	6.78	10.78	2.61	0.40	0.18	1.15	100.05	4.48	7.66	0.507	10.5	
SEG27A-1-1 (Piece 5A, 47–54)	Upper	I-1	49.09	1.95	15.54	11.48	0.18	6.62	11.32	2.56	0.21	0.17	0.87	99.40	4.02	7.75	0.507	12.5	
SEG28A-1-1 (Piece 5, 28–39)	Upper	I-1	47.08	2.06	14.80	12.87	0.22	6.80	10.39	2.78	0.38	0.18	2.45	99.37	5.09	8.14	0.485	1.9	
SEG29A-1-1 (Piece 4B, 26–34)	Upper	I-1	47.84	2.33	14.86	12.66	0.19	7.01	10.21	2.64	0.34	0.20	1.74	99.64	5.94	7.19	0.497	9.8	
SEG31A-1-1 (Piece 1E, 61–68)	Upper	I-1	47.32	2.42	15.12	12.63	0.21	7.09	10.41	2.48	0.22	0.21	1.90	99.55	4.72	8.26	0.500	10.9	
SEG36A-1-1 (Piece 2B, 11–19)	Lower	I-1	46.96	2.23	13.56	12.02	0.20	9.14	10.83	2.39	0.19	0.22	2.26	99.61	6.86	5.72	0.575	6.0	
SEG40A-1-2 (Piece 1, 4–14)	Lower	I-1	47.67	0.83	14.47	10.04	0.17	11.17	11.48	1.63	0.10	0.06	2.38	99.75	5.58	4.94	0.665	14.3	
SEG41A-1-1 (Piece 1C, 16–23)	Lower	I-1	49.13	1.91	14.65	12.26	0.20	6.85	11.30	2.45	0.19	0.18	0.87	99.54	4.39	8.20	0.499	14.4	
SEG42C-1-1 (Piece 5, 41–48)	Lower	I-1	47.11	0.77	16.62	8.73	0.16	9.89	12.39	1.48	0.12	0.07	2.66	99.94	4.87	4.30	0.669	12.7	
SEG43A-1-1 (Piece 4, 11–18)	Lower	I-1	46.16	0.75	16.49	9.16	0.15	10.92	11.29	1.61	0.11	0.06	3.31	99.55	5.19	4.40	0.680	9.9	
SEG44A-1-1 (Piece 1B, 38–46)	Lower	I-1	48.90	2.29	14.16	11.26	0.19	7.49	11.87	2.50	0.22	0.24	0.90	99.73	4.06	7.53	0.542	9.7	
SEG45A-1-1 (Piece 6, 45–49)	Lower	I-1	47.84	1.21	14.86	11.82	0.19	8.50	10.67	2.14	0.19	0.10	2.49	99.88	6.20	6.16	0.561	13.7	
SEG47A-1-1 (Piece 9, 66–74)	Lower	I-1	47.36	2.25	14.05	11.39	0.19	7.78	11.07	2.77	0.38	0.23	2.53	99.80	4.48	7.28	0.549	0.2	
SEG51C-1-1 (Piece 6, 25–32)	Upper	I-1	47.83	3.17	14.27	13.64	0.17	4.99	8.98	3.87	1.18	0.43	1.45	100.07	11.26	3.36	0.395		3.6
SEG52A-1-1 (Piece 2B, 13–20)	Upper	I-1	47.64	2.83	14.10	13.88	0.21	5.84	10.89	2.98	0.41	0.30	0.92	100.06	8.45	6.17	0.428	0.4	
SEG53B-1-1 (Piece 2, 4–11.5)	Upper	I-1	47.94	2.19	14.80	12.35	0.21	6.65	11.34	2.84	0.39	0.23	1.07	99.85	6.56	6.35	0.489		0.1
SEG54A-1-1 (Piece 3, 14–21)	Upper	C-1	48.28	2.66	14.15	13.06	0.22	5.97	11.14	2.94	0.54	0.30	0.75	99.90	6.03	7.54	0.449	0.9	
SEG55B-1-1 (Piece 4, 27–32)	Upper	I-1	48.01	3.01	14.19	12.53	0.21	6.89	10.65	2.94	0.20	0.28	1.07	99.49	5.29	7.64	0.495	6.1	
SEG56A-1-1 (Piece 4, 14–22)	Upper	C-1?	46.79	2.58	14.70	13.09	0.21	6.67	10.35	3.04	0.41	0.23	1.93	99.57	4.81	8.64	0.467		11.1
SEG57A-1-1 (Piece 5, 15–22)	Upper	I-1	45.27	3.62	13.94	14.30	0.22	6.32	10.43	3.09	0.82	0.44	1.55	99.56	7.66	7.23	0.440		4.1
SEG58A-1-1 (Piece 1C, 9–16)	Upper	I-1	48.24	2.84	15.23	12.99	0.19	5.29	10.59	2.73	0.61	0.31	0.98	99.67	5.12	8.27	0.421	9.0	
SEG60B-1-1 (Piece 6A, 90–97)	Upper	I-1	45.08	3.95	13.99	14.63	0.22	6.70	9.50	2.48	0.44	0.37	2.63	99.61	7.90	7.34	0.449	7.9	
SEG61B-1-1 (Piece 1B, 16–23)	Upper	I-1	46.15	2.68	14.42	12.50	0.20	7.05	10.65	2.96	0.51	0.25	2.62	99.43	4.35	8.46	0.501		2.2
SEG61B-1-1 (Piece 8, 95–102)	Upper	I-1	47.03	2.70	14.51	12.60	0.20	7.12	11.00	2.74	0.30	0.25	1.55	99.74	6.20	6.91	0.502	1.1	
SEG62A-1-1 (Piece 2, 13–20)	Upper	I-1	46.32	3.06	14.67	13.25	0.21	6.69	10.35	2.98	0.41	0.29	1.76	99.91	5.66	8.07	0.473		1.0
SEG63A-1-1 (Piece 3, 18–25)	Upper	C-1	46.55	2.61	14.68	12.94	0.20	6.42	11.31	2.85	0.65	0.31	1.48	99.88	8.61	5.06	0.469		2.5
SEG63A-1-1 (???, 18–25)	Upper	C-1	46.96	2.69	14.65	12.70	0.19	6.52	11.28	2.93	0.62	0.30	1.15	99.60	7.12	6.15	0.478		2.3
SEG64B-1-1 (Piece 1, 0–8)	Upper	S-1	46.71	3.69	13.53	14.29	0.23	6.47	10.66	2.68	0.54	0.40	0.81	99.92	3.69	10.90	0.447	2.9	
SEG65B-1-1 (Piece 4, 23–29)	Upper	I-1	47.42	2.16	14.78	11.55	0.19	7.03	12.13	2.68	0.44	0.24	1.37	99.79	5.54	6.48	0.520		1.3
SEG76A-1-1 (Piece 2B, 6.5–11)	Lower	C-1	48.57	2.60	13.10	13.37	0.27	6.58	9.84	3.39	0.37	0.24	1.67	99.62	7.23	6.71	0.467	2.0	
SEG77A-1-1 (Piece 3, 19–26)	Lower	I-1	44.68	2.27	12.86	12.74	0.19	11.48	9.35	1.81	0.59	0.16	3.87	99.41	10.55	3.03	0.616	5.4	

Notes: FeO* = all iron calculated as FeO, Fe_2O_3 and FeO = originally analyzed concentrations. Loss on ignition (LOI) has been corrected for iron oxidation. Major element oxides, including LOI, have been normalized to 100%. Total = sum of oxides as originally analyzed. Mg# = Mg/(Mg + Fe_{total}). CIPW = Cross, Iddings, Pirsson, and Washington normative content (all iron calculated as FeO), Hy = hypersthene, Ne = nepheline.

Table T2 (continued).

Core, section, interval (cm)	Series	Unit	Trace elements (ppm)						
			V	Cr	Ni	Cu	Zn	Sr	Zr
163X-									
SEG21D-1-1 (Piece 1A, 9–18)	Upper	I-1	401	166	70	388	93	250	234
SEG22A-1-1 (Piece 3A, 15–22)	Upper	I-1	410	174	67	335	97	254	245
SEG24A-1-1 (Piece 2, 4–12)	Upper	I-1	322	265	73	161	56	175	120
SEG26A-1-1 (Piece 6G, 85–92)	Upper	I-1	363	198	73	201	71	206	150
SEG27A-1-1 (Piece 5A, 47–54)	Upper	I-1	353	197	72	179	73	212	137
SEG28A-1-1 (Piece 5, 28–39)	Upper	I-1	382	177	67	248	81	317	149
SEG29A-1-1 (Piece 4B, 26–34)	Upper	I-1	385	163	74	198	78	231	175
SEG31A-1-1 (Piece 1E, 61–68)	Upper	I-1	385	179	71	213	84	241	167
SEG36A-1-1 (Piece 2B, 11–19)	Lower	I-1	421	521	280	107	66	229	152
SEG40A-1-2 (Piece 1, 4–14)	Lower	I-1	280	927	385	162	39	55	69
SEG41A-1-1 (Piece 1C, 16–23)	Lower	I-1	395	117	84	219	67	173	141
SEG42C-1-1 (Piece 5, 41–48)	Lower	I-1	251	489	204	98	16	74	72
SEG43A-1-1 (Piece 4, 11–18)	Lower	I-1	217	652	349	110	28	70	58
SEG44A-1-1 (Piece 1B, 38–46)	Lower	I-1	317	298	103	151	61	274	168
SEG45A-1-1 (Piece 6, 45–49)	Lower	I-1	327	379	91	161	41	81	104
SEG47A-1-1 (Piece 9, 66–74)	Lower	I-1	326	315	98	114	64	280	161
SEG51C-1-1 (Piece 6, 25–32)	Upper	I-1	349	46	39	127	102	564	279
SEG52A-1-1 (Piece 2B, 13–20)	Upper	I-1	437	37	29	193	87	321	222
SEG53B-1-1 (Piece 2, 4–11.5)	Upper	I-1	382	117	56	247	69	264	178
SEG54A-1-1 (Piece 3, 14–21)	Upper	C-1	431	61	44	221	78	289	213
SEG55B-1-1 (Piece 4, 27–32)	Upper	I-1	422	188	83	247	90	259	216
SEG56A-1-1 (Piece 4, 14–22)	Upper	C-1?	365	117	69	190	95	317	182
SEG57A-1-1 (Piece 5, 15–22)	Upper	I-1	441	56	58	223	87	528	219
SEG58A-1-1 (Piece 1C, 9–16)	Upper	I-1	335	92	54	260	90	295	235
SEG60B-1-1 (Piece 6A, 90–97)	Upper	I-1	464	146	74	317	105	269	284
SEG61B-1-1 (Piece 1B, 16–23)	Upper	I-1	351	166	88	203	79	401	184
SEG61B-1-1 (Piece 8, 95–102)	Upper	I-1	361	163	91	200	82	271	198
SEG62A-1-1 (Piece 2, 13–20)	Upper	I-1	379	200	88	207	87	292	231
SEG63A-1-1 (Piece 3, 18–25)	Upper	C-1	392	66	57	152	75	336	216
SEG63A-1-1 (???, 18–25)	Upper	C-1	396	71	57	178	77	331	212
SEG64B-1-1 (Piece 1, 0–8)	Upper	S-1	405	161	72	313	106	291	273
SEG65B-1-1 (Piece 4, 23–29)	Upper	I-1	373	92	77	248	65	321	163
SEG76A-1-1 (Piece 2B, 6.5–11)	Lower	C-1	402	88	52	228	85	172	182
SEG77A-1-1 (Piece 3, 19–26)	Lower	I-1	363	602	349	146	71	220	147

Table T3. Summary of phenocryst composition, Transect EG65.

Core, section, interval (cm)	Series	Plagioclase (An mol%)		Augite (Mg#)		Olivine (Fo mol%)		Chromian spinel (Cr#)	
		Average	Range	Average	Range	Average	Range	Average	Range
163X-									
SEG21D-1-1 (Piece 1A, 9–13)	Upper	65	64–66	75	73–77	—	—	—	—
SEG22A-1-1 (Piece 3A, 15–19)	Upper	65	64–66	76	74–77	—	—	—	—
SEG24A-1-1 (Piece 1, 0–4)	Upper	76	73–78	75	75–76	—	—	—	—
SEG24A-1-1 (Piece 2, 4–8)	Upper	86	84–87	81	78–83	—	—	—	—
SEG26A-1-1 (Piece 6G, 85–89)	Upper	77	75–79	76	75–77	—	—	—	—
SEG27A-1-1 (Piece 5A, 47–51)	Upper	72	70–74	78	77–79	—	—	—	—
SEG28A-1-1 (Piece 5, 28–32)	Upper	70	67–72	78	77–79	—	—	—	—
SEG29A-1-1 (Piece 4B, 26–30)	Upper	—	—	75	74–77	—	—	—	—
SEG31A-1-1 (Piece 1E, 61–65)	Upper	71	69–74	76	73–78	—	—	—	—
SEG36A-1-1 (Piece 2B, 11–15)	Lower	—	—	—	—	—	—	—	—
SEG40A-1-2 (Piece 1, 10–14)	Lower	87	86–88	—	—	—	—	0.524	0.518–0.534
SEG41A-1-1 (Piece 1C, 16–20)	Lower	79	78–80	77	74–80	—	—	—	—
SEG42B-1-1 (Piece 2, 7–8)	Lower	89	89–90	—	—	—	—	—	—
SEG42C-1-1 (Piece 5, 41–45)	Lower	83	79–87	85	84–86	—	—	—	—
SEG43A-1-1 (Piece 4, 11–15)	Lower	87	85–89	—	—	—	—	0.449	0.445–0.454
SEG44A-1-1 (Piece 1B, 39–42)	Lower	—	—	—	—	75	68–76	0.422	0.418–0.426
SEG45A-1-1 (Piece 6, 45–49)	Lower	76	75–77	82	80–83	—	—	—	—
SEG47A-1-1 (Piece 9, 70–74)	Upper	—	—	—	—	—	—	—	—
SEG51C-1-1 (Piece 6, 25–29)	Upper	58	57–60	71	68–77	—	—	—	—
SEG52A-1-1 (Piece 2B, 16–20)	Upper	—	—	76	72–78	—	—	—	—
SEG53B-1-1 (Piece 2, 85–115)	Upper	77	76–78	77	64–80	—	—	—	—
SEG54A-1-1 (Piece 3, 14–18)	Upper	82	80–83	78	74–80	—	—	—	—
SEG55B-1-1 (Piece 4, 27–31)	Upper	75	70–78	—	—	—	—	—	—
SEG56A-1-1 (Piece 4, 14–18)	Upper	71	69–73	—	—	69	68–70	—	—
SEG57A-1-1 (Piece 5, 18–22)	Upper	67	64–71	—	—	62	60–67	—	—
SEG58A-1-1 (Piece 1C, 9–13)	Upper	66	65–67	73	72–74	61	58–65	—	—
SEG60B-1-1 (Piece 6A, 93–97)	Upper	64	60–67	79	75–80	—	—	—	—
SEG61B-1-1 (Piece 1B, 19–23)	Upper	63	56–70	75	74–76	54	52–56	—	—
SEG61B-1-1 (Piece 8, 95–99)	Upper	65	63–66	76	75–77	68	65–71	—	—
SEG62A-1-1 (Piece 2, 13–17)	Upper	69	67–71	77	76–78	—	—	—	—
SEG63A-1-1 (Piece 3, 18–20)	Upper	78	77–78	77	73–80	—	—	—	—
SEG64B-1-1 (Piece 1, 0–4)	Upper	67	65–69	70	66–72	69	63–70	—	—
SEG65B-1-1 (Piece 4, 23–24)	Upper	—	—	—	—	—	—	—	—
SEG76A-1-1 (Piece 2B, 8–10)	Lower	68	68	—	—	—	—	—	—
SEG76B-1-1 (Piece 3, 18–19)	Lower	—	—	—	—	68	—	0.592	0.585–0.605
SEG77A-1-1 (Piece 3, 22–26)	Lower	—	—	—	—	—	—	0.568	0.503–0.658

Notes: See **"Appendix B,"** p. 13, in the "Explanatory Notes" chapter for details. An = anorthite, Fo = forsterite. Mg# = 100 × Mg/(Mg + Fe) with all iron as Fe^{2+}, Cr# = Cr/(Cr + Al + Fe^{3+}). Gneiss (Sample 163X-SEG32A-1-1 [Piece 2B, 21–23 cm] and sandstone (Samples 163X-SEG38B-1-1 [Piece 2, 8–12 cm] and 163X-SEG80B-1-1 [Piece 2, 39–42 cm]) thin sections were prepared but not listed here. — = phase not present, not analyzed, or replaced by secondary materials.

Table T4. Paleomagnetic results, Transect EG65.

Core, section, interval (cm)	NRM (nA/m)	χ (10^{-3} SI)	Q ratio	CI (°)	Polarity	Comments
163X-						
SEG21A-1-1 (Piece 4A, 11–14)	779	13.76	1.41	–77.2	R	
SEG21D-1-1 (Piece 1A, 2–5)	1,112	10.12	2.75	–81.5	R	
SEG22A-1-1 (Piece 3A, 25–28)	6,448	12.54	12.85	–43.9	R	
SEG22A-1-1 (Piece 6, 72–75)	3,234	18.08	4.47	–55.3	R	
SEG23A-1-1 (Piece 2, 6–9)	1,158	9.36	3.09	–54	R	
SEG24A-1-1 (Piece 2, 48–51)	3,993	21.86	4.57	–71.7	R	
SEG26A-1-1 (Piece 4E, 29–32)	1,749	32.20	1.36	–66	R	
SEG26A-1-2 (Piece 1C, 15–18)	3,004	38.52	1.95	–54.7	R	
SEG27A-1-1 (Piece 5A, 45–48)	2,346	14.80	3.96	–37.5	R	
SEG27A-1-2 (Piece 3B, 45–48)	1,966	24.48	2.01	–39.5	R	
SEG28A-1-1 (Piece 4, 24–27)	5,413	21.12	6.41	–54.6	R	
SEG29A-1-1 (Piece 4A, 23–26)	8,412	50.30	4.18	–64.1	R	
SEG31A-1-1 (Piece 1D, 50–53)	3,701	16.00	5.78	–56.6	R	
SEG36A-1-1 (Piece 2C, 18–21)	3,273	15.60	5.25	–72.6	R	
SEG39A-1-1 (Piece 2, 7–10)	2,133	19.36	2.75	35.4	?	Clast
SEG40A-1-1 (Piece 1A, 7–10)	3,266	22.78	3.58	–71.5	R	
SEG40A-1-2 (Piece 1, 29–32)	5,802	16.40	8.84	–71.1	R	
SEG41A-1-1 (Piece 1C, 8–11)	3,205	32.80	2.44	?	?	Not defined
SEG42A-1-1 (Piece 3, 11–14)	1,310	2.90	11.29	–40.8	R	
SEG42B-1-1 (Piece 4, 33–36)	7,451	23.72	7.85	–66.7	R	
SEG42C-1-1 (Piece 2C, 25–28)	11,780	30.76	9.57	–59.4	R	
SEG43A-1-1 (Piece 6, 23–26)	2,193	5.68	9.65	–54.5	R	
SEG44A-1-1 (Piece 1B, 13–16)	1,425	14.08	2.53	–4.1	E (?)	
SEG45A-1-1 (Piece 2, 21–24)	4,337	13.66	7.94	–28.4	E (?)	
SEG47A-1-1 (Piece 4, 26–29)	408	10.90	0.93	–65.5	R	
SEG51C-1-1 (Piece 7, 39–42)	1,241	76.25	0.41	–58.8	R	
SEG52A-1-1 (Piece 2C, 27–30)	7,656	33.75	5.67	–74	R	
SEG53B-1-1 (Piece 4A, 18–21)	4,574	33.32	3.43	–62.3	R	
SEG54A-1-1 (Piece 2, 7–10)	1,442	53.25	0.68	–57.5	R	
SEG55B-1-1 (Piece 2, 19–22)	6,183	16.40	9.43	–60	R	
SEG55C-1-1 (Piece 2, 10–13)	5,562	64.60	2.15	64.2	?	Turned?
SEG56A-1-1 (Piece 7, 32–35)	2,716	14.70	4.62	–77.4	R	
SEG57A-1-1 (Piece 7B, 33–36)	3,048	54.95	1.39	–82.8	R	
SEG58A-1-1 (Piece 1A, 5–8)	3,949	24.70	4.00	–71.2	R	
SEG60B-1-1 (Piece 3B, 48–51)	1,481	34.50	1.07	–65.1	R	
SEG61A-1-1 (Piece 4A, 36–39)	6,121	18.75	8.16	–48.4	R	
SEG61A-1-1 (Piece 4L, 55–58)	6,328	19.35	8.18	–38.9	R	
SEG61B-1-1 (Piece 8, 94–97)	5,588	15.10	9.25	–45.6	R	
SEG61B-1-2 (Piece 2F, 53–56)	7,028	21.05	8.35	–50.1	R	
SEG62A-1-1 (Piece 4, 22–25)	1,333	32.60	1.02	–55.5	R	
SEG63B-1-1 (Piece 4, 14–17)	809	55.75	0.36	–58.6	R	
SEG65B-1-1 (Piece 2E, 14–17)	2,625	25.35	2.59	–78.2	R	
SEG74E-1-1 (Piece 1, 4–7)	4,996	34.80	3.59	–15.2	E (?)	
SEG75A-1-1 (Piece 2, 18–21)	2,483	17.30	3.59	–66.9	R	
SEG75B-1-1 (Piece 5A, 17–20)	2,469	15.15	4.07	–64.5	R	
SEG75C-1-1 (Piece 3, 29–32)	5,055	20.30	6.23	–67.9	R	
SEG76A-1-1 (Piece 2A, 3–6)	4,319	27.60	3.91	–9.3	E (?)	
SEG77A-1-1 (Piece 5A, 43–46)	6,507	12.20	13.33	–37.3	R	
SEG77B-1-1 (Piece 2, 7–10)	2,288	15.10	3.79	–24.9	R	Drill tipped
SEG79C-1-1 (Piece 3, 19–22)	2,392	39.60	1.51	?	?	Not defined

Notes: NRM = natural remanent magnetization, χ = magnetic susceptibility, Q ratio = Königsberger ratio, CI = characteristic inclination. R = reversed, E = excursion event, ? = unknown.